fractal and fractional

Article

Solving General Fractional Lane-Emden-Fowler Differential Equations Using Haar Wavelet Collocation Method

Kholoud Saad Albalawi [1], Ashish Kumar [2,*], Badr Saad Alkahtani [3] and Pranay Goswami [2]

[1] Department of Mathematics and Statistics, College of Science, Imam Mohammad Ibn Saud Islamic University, Riyadh 11566, Saudi Arabia; ksalbalawi@imamu.edu.sa
[2] School of Liberal Studies, Dr. B.R. Ambedkar University Delhi, Delhi 110006, India; pranaygoswami83@gmail.com
[3] Department of Mathematics, College of Science, King Saud University, Riyadh 11989, Saudi Arabia; balqahtani1@ksu.edu.sa
* Correspondence: ashish4747.ak@gmail.com

Abstract: This paper aims to solve general fractional Lane-Emden-Fowler differential equations using the Haar wavelet collocation method. This method transforms the fractional differential equation into a nonlinear system of equations, which is further solved for Haar coefficients using Newton's method. We have constructed the higher-order Lane-Emden-Fowler equations. We have also discussed the convergence rate and stability analysis of our technique. We have explained the applications and numerically simulated the examples graphically and in tabular format to elaborate on the accuracy and efficiency of this approach.

Keywords: fractional differential equations; Lane-Emden-Fowler type equations; numerical method; Haar wavelet collection method

MSC: 34A08; 65L60; 65T60; 26A33

check for updates

Citation: Albalawi, K.S.; Kumar, A.; Alkahtani, B.S.; Goswami, P. Solving General Fractional Lane-Emden-Fowler Differential Equations Using Haar Wavelet Collocation Method. *Fractal Fract.* **2023**, *7*, 628. https://doi.org/10.3390/fractalfract7080628

Academic Editor: Peter Massopust

Received: 20 July 2023
Revised: 13 August 2023
Accepted: 15 August 2023
Published: 17 August 2023

1. Introduction

In the past few decades, the study of singular initial value problems has attracted the attention of many physicists and mathematicians. Lane-Emden-Fowler equations are these types of equations. Lane [1] introduced the equation in 1870, and Emden and Fowler [2] generalized the equation further. Lane explained the gravitation potential of a spherically symmetric Newtonian self-gravitating star [3] using these equations. These equations have a vast amount of applications in modeling many problems in physics and dynamics. The general Lane-Emden-Fowler equation is as follows:

$$\xi^{-\eta} D^{\beta}(\xi^{\eta} D^{\gamma})q = \omega(\xi, q(\xi)), \tag{1}$$

where $\eta > 0$ is a positive real number called a shape factor, $D = \frac{d}{d\xi}$ is the differential operator, ω is linear or nonlinear function, and $\beta + \gamma$ gives the order of the equation. These equations are used in magnetic field models [4], classical and quantum mechanics [5], biological systems, geometry [6], and fluid mechanics problems [7,8].

Several forms of fractional initial value problems have been proposed in standard models, and there has been a significant interest in developing numerical schemes for their solutions. Fractional calculus is a generalized form of integer order calculus. There are many applications of fractional calculus. Fractional calculus has been deployed to model the oscillation of earthquakes [9], neural networks [10,11], signal processing [12], economics [13], bioengineering [14], and electromagnetism [15].

Many researchers, such as Riemann, Liouville, Caputo, Hadamard, Grunwald, and others, have published extensively about the applications of fractional calculus. Mathematical models with fractional order derivatives provide more insight because they posses the memory effect. Many techniques have been developed to solve fractional problems, such as decomposition methods [16], collocation methods [17], residual power series methods [18,19], finite differences methods [20], perturbation methods, variational iteration methods [21]. Zhang and Han [22] proposed a quasi wavelet method to solve time-dependent fractional partial differential equations. Jiang et al. [23] presented a predictor–corrector difference scheme for nonlinear fractional differential equations. Yang and Zhang [24] proposed a spectral sinc-collocation method for fourth-order heat models.

Wavelet theory has made distinguished contributions to mathematical studies. It is a powerful tool for engineering. Wavelets are used in signal processing, optimal control, and time-frequency analysis [25]. There are many wavelets, such as Daubechies [26], B-spline [4], Legendre [27], and Haar [28]. The Haar wavelet is an orthonormal wavelet with compact support, introduced by a Hungarian mathematician, Alfred Haar, in 1910. The Haar wavelet gives accurate results for small grid points. It contains members of the Daubechies family, so it is very good for computer implementations and is easily expressed in the programming language. Chen and Hsiao [29] derived a Haar operational matrix of the integrals of Haar functions. They made a great contribution to the use of Haar wavelets in applications of dynamic systems. Lepik [30] solved the differential equations using the Haar wavelet. Islam et al. [31] solved the integro-differential equations using the Haar wavelet. Bujurke et al. [32] compute the eigenvalues and solutions of regular Sturm–Liouville problems using Haar wavelets. Chang et al. [33] describe the designation of Haar wavelet matrices in the numerical solution of ODEs. This article aims to solve general fractional Emden-Fowler-type equations using the Haar wavelet collocation method. We write the highest derivative in linear combinations of Haar functions and calculate other derivatives using the integration of Haar functions. This method transforms the fractional differential equation into a nonlinear system of equations, which is further solved for Haar coefficients using the Newton method. After calculating the Haar coefficients, we can easily determine the solution.

The present study is structured as follows: Section 2 defines the Haar wavelet and recalls the basic definitions of fractional calculus. In Section 3, we discuss the construction of the general equation of the Caputo-type fractional Lane-Emden-Fowler differential equation. In Section 4, we discuss the Haar wavelet method. In Section 5, we discuss the convergence rate, stability and error analysis of the technique. In Section 6, we discuss the examples and in Section 7 we discuss the numerical simulation of all of these examples graphically and in tabular format. In the end, we conclude our results.

2. Preliminaries

This section will recall some necessary definitions of fractional calculus and Haar wavelets. These definitions will assist us in the next sections.

Definition 1. *The Riemann-Liouville fractional integral operator I^{σ} of order σ on $L_2[0,1]$ is given by*

$$I^{\sigma}(q(\xi)) = \frac{1}{\Gamma(\sigma)}\int_0^{\xi} \frac{q(\kappa)}{(\xi-\kappa)^{1-\sigma}}d\kappa,$$
$$I^{0}(q(\xi)) = (q(\xi)),$$

where $\Gamma(\lambda) = \int_0^{\infty} \kappa^{\lambda-1}e^{-\kappa}d\kappa$ is gamma function and

$$I^{\sigma}\xi^{v} = \frac{\Gamma(v+1)}{\Gamma(\sigma+v+1)}\xi^{\sigma+v}.$$

Definition 2. *The Caputo fractional derivative of order σ is given by*

$$D^{\sigma}(q(\xi)) = I^{n-\sigma}D^{n}(q(\xi)) = \frac{1}{\Gamma(n-\sigma)}\int_{0}^{\xi}\frac{q^{(n)}(\kappa)}{(\xi-\kappa)^{-n+1+\sigma}}d\kappa$$

provided the integral exists, where n is the smallest integer such that $n-1<\sigma\leq n$. It satisfies the following properties:

$$I^{\sigma}D^{\sigma}(q(\xi)) = q(\xi) - \sum_{\varepsilon=0}^{n-1} q^{(\varepsilon)}(0^{+})\frac{\xi^{\varepsilon}}{\varepsilon!}$$

and

$$D^{\sigma}\xi^{v} = \frac{\Gamma(v+1)}{\Gamma(v-\sigma+1)}\xi^{v-\sigma}.$$

Haar Wavelet and Function Approximations

The family of Haar wavelets consists of piecewise constant functions over the real line. They contain only values $-1,0,1$. They are discontinuous, and therefore not differentiable.

$$h_j(\varsigma) = \begin{cases} 1, & \theta_1(j) \leq \varsigma < \theta_2(j) \\ -1, & \theta_2(j) \leq \varsigma < \theta_3(j) \\ 0, & otherwise. \end{cases}$$

where $\theta_1(j) = \frac{r}{2^{\alpha}}, \theta_2(j) = \frac{r+0.5}{2^{\alpha}}, \theta_3(j) = \frac{r+1}{2^{\alpha}}$, $\alpha = 0,1,2,\ldots J$ and $r = 0,1,2,\ldots 2^{\alpha}-1$.

We manipulate the wavelet by translating and dilating it. α here represents the level of wavelet or dilation parameter level and ς represents the translation parameter. J is the maximum level of resolution and the relationship between 2^{α} and r is $j = 2^{\alpha}+r+1$. For $j=1$

$$h_1(\xi) = \begin{cases} 1, & \xi \in [0,1] \\ 0, & otherwise. \end{cases}$$

$$h_2(\xi) = \begin{cases} 1, \xi \in \left[0,\frac{1}{2}\right) \\ -1, \xi \in \left[\frac{1}{2},1\right) \\ 0, otherwise. \end{cases}$$

In particular, the Haar wavelet is an orthogonal square wave family, generally written as

$$h_j(\xi) = h_2\left(2^{\alpha}\xi - \frac{r}{2^{\alpha}}\right)$$

for $j\geq 3, j = 2^{\alpha}+r+1, \alpha\geq 0, 0\leq r\leq 2^{\alpha}-1$ and

$$\int_{0}^{1} h_j(\xi)h_l(\xi)d\xi = \begin{cases} 2^{-\alpha}; j = l \\ 0; j\neq l \end{cases}$$

If $g(\xi)$ is a function defined on interval $[0,1]$, then the function is approximated using Haar functions, such as

$$g(\xi) = \sum_{\tau=1}^{\infty}\lambda_{\tau}h_{\tau},$$

where λ_{τ} are the Haar coefficients.

The generalized fractional integration can be calculated analytically as

$$\rho_{\tau,\sigma}(\xi) = \begin{cases} 0, \xi \in [0, \varsigma_1) \\ \frac{1}{\Gamma(\sigma+1)}(\xi - \varsigma_1)^{\sigma}, \xi \in [\varsigma_1, \varsigma_2) \\ \frac{1}{\Gamma(\sigma+1)}\left[(\xi - \varsigma_1)^{\sigma} - 2(\xi - \varsigma_2)^{\sigma}\right], \xi \in [\varsigma_2, \varsigma_3) \\ \frac{1}{\Gamma(\sigma+1)}\left[(\xi - \varsigma_1)^{\sigma} - 2(\xi - \varsigma_2)^{\sigma} + (\xi - \varsigma_3)^{\sigma}\right], \xi \in [\varsigma_3, 1) \end{cases},$$

where σ is a positive real number.

3. Construction of Lane-Emden-Fowler Equation

Consider the general form of the Lane-Emden-Fowler equation

$$\xi^{-\eta} D^{\beta}(\xi^{\eta} D^{\gamma})q = \omega(\xi, q(\xi)). \tag{2}$$

We can obtain higher-order equations of fourth-, fifth- and sixth-order by taking

$$\beta + \gamma = 4,$$

$$\beta + \gamma = 5,$$

$$\beta + \gamma = 6,$$

respectively. There are three possible choices of fourth-order equations, four possibilities for fifth-order equations and five possible choices for sixth-order Lane-Emden-Fowler equations.

3.1. For Fourth-Order Equations

Case 1: When $\beta = 3$, $\gamma = 1$, the equation will be

$$\xi^{-\eta} D^{3}\left(\xi^{\eta} D^{1}\right)q + \omega(\xi, q(\xi)) = 0. \tag{3}$$

After simplification, Equation (3) will be

$$D^4 q(\xi) + \frac{3\eta}{\xi} D^3 q(\xi) + \frac{3\eta(\eta-1)}{\xi^2} D^2 q(\xi) + \frac{\eta(\eta-1)(\eta-2)}{\xi^3} Dq(\xi) + \omega(\xi, q(\xi)) = 0. \tag{4}$$

The Equation (4) in fractional order is taken as

$$D^{4\sigma} q(\xi) + \frac{3\eta}{\xi^{\sigma}} D^{3\sigma} q(\xi) + \frac{3\eta(\eta-1)}{\xi^{2\sigma}} D^{2\sigma} q(\xi) + \frac{\eta(\eta-1)(\eta-2)}{\xi^{3\sigma}} D^{\sigma} q(\xi) + \omega(\xi, q(\xi)) = 0, \tag{5}$$

with initial conditions $q(0) = \phi_0, q^{(\sigma)}(0) = \phi_1, q^{(2\sigma)}(0) = \phi_2, q^{(3\sigma)}(0) = \phi_3$, where $q^{(\sigma)}, q^{(2\sigma)}, q^{(3\sigma)}$ denotes the Caputo derivative of order $\sigma, 2\sigma, 3\sigma$, respectively.

Case 2: When $\beta = 2$, $\gamma = 2$, the equation will be

$$\xi^{-\eta} D^{2}\left(\xi^{\eta} D^{2}\right)q + \omega(\xi, q(\xi)) = 0. \tag{6}$$

After simplification, Equation (6) will be

$$D^4 q(\xi) + \frac{2\eta}{\xi} D^3 q(\xi) + \frac{\eta(\eta-1)}{\xi^2} D^2 q(\xi) + \omega(\xi, q(\xi)) = 0. \tag{7}$$

The Equation (7) in fractional order is taken as

$$D^{4\sigma} q(\xi) + \frac{2\eta}{\xi^{\sigma}} D^{3\sigma} q(\xi) + \frac{\eta(\eta-1)}{\xi^{2\sigma}} D^{2\sigma} q(\xi) + \omega(\xi, q(\xi)) = 0. \tag{8}$$

with initial conditions $q(0) = \phi_0, q^{(\sigma)}(0) = \phi_1, q^{(2\sigma)}(0) = \phi_2, q^{(3\sigma)}(0) = \phi_3$, where $q^{(\sigma)}, q^{(2\sigma)}, q^{(3\sigma)}$ denotes the Caputo derivative of order $\sigma, 2\sigma, 3\sigma$, respectively.

Case 3: When $\beta = 1, \gamma = 3$, the equation will be

$$\xi^{-\eta} D^1 \left(\xi^{\eta} D^3\right) q + \omega(\xi, q(\xi)) = 0. \tag{9}$$

After simplification, Equation (9) will be

$$D^4 q(\xi) + \frac{\eta}{\xi} D^3 q(\xi) + \omega(\xi, q(\xi)) = 0. \tag{10}$$

The Equation (10) in fractional order is taken as

$$D^{4\sigma} q(\xi) + \frac{\eta}{\xi^{\sigma}} D^{3\sigma} q(\xi) + \omega(\xi, q(\xi)) = 0. \tag{11}$$

with initial conditions $q(0) = \phi_0, q^{(\sigma)}(0) = \phi_1, q^{(2\sigma)}(0) = \phi_2, q^{(3\sigma)}(0) = \phi_3$, where $q^{(\sigma)}, q^{(2\sigma)}, q^{(3\sigma)}$ denotes the Caputo derivative of order $\sigma, 2\sigma, 3\sigma$, respectively.

3.2. For Fifth-Order Equations

Case 1: When $\beta = 4, \gamma = 1$, the equation will be

$$\xi^{-\eta} D^4 \left(\xi^{\eta} D^1\right) q + \omega(\xi, q(\xi)) = 0. \tag{12}$$

After simplification, Equation (12) will be

$$\begin{aligned} &D^5 q(\xi) + \tfrac{4\eta}{\xi} D^4 q(\xi) + \tfrac{6\eta(\eta-1)}{\xi^2} D^3 q(\xi) + \tfrac{4\eta(\eta-1)(\eta-2)}{\xi^3} D^2 q(\xi) \\ &+ \tfrac{\eta(\eta-1)(\eta-2)(\eta-3)}{\xi^4} D q(\xi) + \omega(\xi, q(\xi)) = 0. \end{aligned} \tag{13}$$

The Equation (13) in fractional order is taken as

$$\begin{aligned} &D^{5\sigma} q(\xi) + \tfrac{4\eta}{\xi^{\sigma}} D^{4\sigma} q(\xi) + \tfrac{6\eta(\eta-1)}{\xi^{2\sigma}} D^{3\sigma} q(\xi) + \tfrac{4\eta(\eta-1)(\eta-2)}{\xi^{3\sigma}} D^{2\sigma} q(\xi) \\ &+ \tfrac{\eta(\eta-1)(\eta-2)(\eta-3)}{\xi^{4\sigma}} D^{\sigma} q(\xi) + \omega(\xi, q(\xi)) = 0, \end{aligned} \tag{14}$$

with initial conditions $q(0) = \phi_0, q^{(\sigma)}(0) = \phi_1, q^{(2\sigma)}(0) = \phi_2, q^{(3\sigma)}(0) = \phi_3, q^{(4\sigma)}(0) = \phi_4$, where $q^{(\sigma)}, q^{(2\sigma)}, q^{(3\sigma)}, q^{(4\sigma)}$ denotes the Caputo derivative of order $\sigma, 2\sigma, 3\sigma, 4\sigma$, respectively.

Case 2: When $\beta = 3, \gamma = 2$, the equation will be

$$\xi^{-\eta} D^3 \left(\xi^{\eta} D^2\right) q + \omega(\xi, q(\xi)) = 0. \tag{15}$$

After simplification, Equation (15) will be

$$D^5 q(\xi) + \frac{3\eta}{\xi} D^4 q(\xi) + \frac{3\eta(\eta-1)}{\xi^2} D^3 q(\xi) + \frac{\eta(\eta-1)(\eta-2)}{\xi^3} D^2 q(\xi) + \omega(\xi, q(\xi)) = 0. \tag{16}$$

The Equation (16) in fractional order is taken as

$$D^{5\sigma} q(\xi) + \tfrac{3\eta}{\xi^{\sigma}} D^{4\sigma} q(\xi) + \tfrac{3\eta(\eta-1)}{\xi^{2\sigma}} D^{3\sigma} q(\xi) + \tfrac{\eta(\eta-1)(\eta-2)}{\xi^{3\sigma}} D^{2\sigma} q(\xi) + \omega(\xi, q(\xi)) = 0. \tag{17}$$

with initial conditions $q(0) = \phi_0, q^{(\sigma)}(0) = \phi_1, q^{(2\sigma)}(0) = \phi_2, q^{(3\sigma)}(0) = \phi_3, q^{(4\sigma)}(0) = \phi_4$, where $q^{(\sigma)}, q^{(2\sigma)}, q^{(3\sigma)}, q^{(4\sigma)}$ denotes the Caputo derivative of order $\sigma, 2\sigma, 3\sigma, 4\sigma$, respectively.

Case 3: When $\beta = 2, \gamma = 3$, the equation will be

$$\xi^{-\eta} D^2 \left(\xi^{\eta} D^3\right) q + \omega(\xi, q(\xi)) = 0. \tag{18}$$

After simplification, Equation (18) will be

$$D^5 q(\xi) + \frac{2\eta}{\xi} D^4 q(\xi) + \frac{\eta(\eta-1)}{\xi^2} D^3 q(\xi) + \omega(\xi, q(\xi)) = 0. \tag{19}$$

The Equation (19) in fractional order is taken as

$$D^{5\sigma} q(\xi) + \frac{2\eta}{\xi^\sigma} D^{4\sigma} q(\xi) + \frac{\eta(\eta-1)}{\xi^{2\sigma}} D^{3\sigma} q(\xi) + \omega(\xi, q(\xi)) = 0, \tag{20}$$

with initial conditions $q(0) = \phi_0, q^{(\sigma)}(0) = \phi_1, q^{(2\sigma)}(0) = \phi_2, q^{(3\sigma)}(0) = \phi_3, q^{(4\sigma)}(0) = \phi_4$, where $q^{(\sigma)}, q^{(2\sigma)}, q^{(3\sigma)}, q^{(4\sigma)}$ denotes the Caputo derivative of order σ, 2σ, 3σ, 4σ, respectively.

Case 4: When $\beta = 1$, $\gamma = 4$, the equation will be

$$\xi^{-\eta} D^1 \left(\xi^\eta D^4\right) q + \omega(\xi, q(\xi)) = 0. \tag{21}$$

After simplification, Equation (21) will be

$$D^5 q(\xi) + \frac{\eta}{\xi} D^4 q(\xi) + \omega(\xi, q(\xi)) = 0. \tag{22}$$

The Equation (22) in fractional order is taken as

$$D^{5\sigma} q(\xi) + \frac{\eta}{\xi^\sigma} D^{4\sigma} q(\xi) + \omega(\xi, q(\xi)) = 0. \tag{23}$$

with initial conditions $q(0) = \phi_0, q^{(\sigma)}(0) = \phi_1, q^{(2\sigma)}(0) = \phi_2, q^{(3\sigma)}(0) = \phi_3, q^{(4\sigma)}(0) = \phi_4$, where $q^{(\sigma)}, q^{(2\sigma)}, q^{(3\sigma)}, q^{(4\sigma)}$ denotes the Caputo derivative of order σ, 2σ, 3σ, 4σ, respectively.

3.3. For Sixth-Order Equations

Case 1: When $\beta = 5$, $\gamma = 1$, the equation will be

$$\xi^{-\eta} D^5 \left(\xi^\eta D^1\right) q + \omega(\xi, q(\xi)) = 0. \tag{24}$$

After simplification, Equation (24) will be

$$\begin{aligned} &D^6 q(\xi) + \tfrac{4\eta}{\xi} D^5 q(\xi) + \tfrac{10\eta(\eta-1)}{\xi^2} D^4 q(\xi) + \tfrac{10\eta(\eta-1)(\eta-2)}{\xi^3} D^3 q(\xi) \\ &+ \tfrac{5\eta(\eta-1)(\eta-2)(\eta-3)}{\xi^4} D^2 q(\xi) + \tfrac{\eta(\eta-1)(\eta-2)(\eta-3)(\eta-4)}{\xi^5} D q(\xi) + \omega(\xi, q(\xi)) = 0. \end{aligned} \tag{25}$$

The Equation (25) in fractional order is taken as

$$\begin{aligned} &D^{6\sigma} q(\xi) + \tfrac{4\eta}{\xi^\sigma} D^{5\sigma} q(\xi) + \tfrac{10\eta(\eta-1)}{\xi^{2\sigma}} D^{4\sigma} q(\xi) + \tfrac{10\eta(\eta-1)(\eta-2)}{\xi^{3\sigma}} D^{3\sigma} q(\xi) \\ &+ \tfrac{5\eta(\eta-1)(\eta-2)(\eta-3)}{\xi^{4\sigma}} D^{2\sigma} q(\xi) + \tfrac{\eta(\eta-1)(\eta-2)(\eta-3)(\eta-4)}{\xi^{5\sigma}} D^{\sigma} q(\xi) + \omega(\xi, q(\xi)) = 0, \end{aligned} \tag{26}$$

with initial conditions $q(0) = \phi_0, q^{(\sigma)}(0) = \phi_1, q^{(2\sigma)}(0) = \phi_2, q^{(3\sigma)}(0) = \phi_3, q^{(4\sigma)}(0) = \phi_4$, $q^{(5\sigma)}(0) = \phi_5$, where $q^{(\sigma)}, q^{(2\sigma)}, q^{(3\sigma)}, q^{(4\sigma)}, q^{(5\sigma)}$ denotes the Caputo derivative of order σ, 2σ, 3σ, 4σ, 5σ, respectively.

Case 2: When $\beta = 4$, $\gamma = 2$, the equation will be

$$\xi^{-\eta} D^4 \left(\xi^\eta D^2\right) q + \omega(\xi, q(\xi)) = 0. \tag{27}$$

After simplification, Equation (27) will be

$$\begin{aligned} &D^6 q(\xi) + \tfrac{4\eta}{\xi} D^5 q(\xi) + \tfrac{6\eta(\eta-1)}{\xi^2} D^4 q(\xi) + \tfrac{4\eta(\eta-1)(\eta-2)}{\xi^3} D^3 q(\xi) \\ &+ \tfrac{\eta(\eta-1)(\eta-2)(\eta-3)}{\xi^4} D^2 q(\xi) + \omega(\xi, q(\xi)) = 0. \end{aligned} \tag{28}$$

The Equation (28) in fractional order is taken as

$$D^{6\sigma}q(\xi)+\frac{4\eta}{\xi^{\sigma}}D^{5\sigma}q(\xi)+\frac{6\eta(\eta-1)}{\xi^{2\sigma}}D^{4\sigma}q(\xi)+\frac{4\eta(\eta-1)(\eta-2)}{\xi^{3\sigma}}D^{3\sigma}q(\xi) \\ +\frac{\eta(\eta-1)(\eta-2)(\eta-3)}{\xi^{4\sigma}}D^{2\sigma}q(\xi)+\omega(\xi,q(\xi))=0. \tag{29}$$

with initial conditions $q(0)=\phi_0, q^{(\sigma)}(0)=\phi_1, q^{(2\sigma)}(0)=\phi_2, q^{(3\sigma)}(0)=\phi_3, q^{(4\sigma)}(0)=\phi_4$, $q^{(5\sigma)}(0)=\phi_5$, where $q^{(\sigma)}, q^{(2\sigma)}, q^{(3\sigma)}, q^{(4\sigma)}, q^{(5\sigma)}$ denotes the Caputo derivative of order σ, 2σ, 3σ, 4σ, 5σ, respectively.

Case 3: When $\beta=3$, $\gamma=3$, the equation will be

$$\xi^{-\eta}D^3\left(\xi^{\eta}D^3\right)q+\omega(\xi,q(\xi))=0. \tag{30}$$

After simplification, Equation (30) will be

$$D^6q(\xi)+\frac{3\eta}{\xi}D^5q(\xi)+\frac{3\eta(\eta-1)}{\xi^2}D^4q(\xi)+\frac{\eta(\eta-1)(\eta-2)}{\xi^3}D^3q(\xi)+\omega(\xi,q(\xi))=0. \tag{31}$$

The Equation (31) in fractional order is taken as

$$D^{6\sigma}q(\xi)+\frac{3\eta}{\xi^{\sigma}}D^{5\sigma}q(\xi)+\frac{3\eta(\eta-1)}{\xi^{2\sigma}}D^{4\sigma}q(\xi)+\frac{\eta(\eta-1)(\eta-2)}{\xi^{3\sigma}}D^{3\sigma}q(\xi)+\omega(\xi,q(\xi))=0. \tag{32}$$

with initial conditions $q(0)=\phi_0, q^{(\sigma)}(0)=\phi_1, q^{(2\sigma)}(0)=\phi_2, q^{(3\sigma)}(0)=\phi_3, q^{(4\sigma)}(0)=\phi_4$, $q^{(5\sigma)}(0)=\phi_5$, where $q^{(\sigma)}, q^{(2\sigma)}, q^{(3\sigma)}, q^{(4\sigma)}, q^{(5\sigma)}$ denotes the Caputo derivative of order σ, 2σ, 3σ, 4σ, 5σ, respectively.

Case 4: When $\beta=2$, $\gamma=4$, the equation will be

$$\xi^{-\eta}D^2\left(\xi^{\eta}D^4\right)q+\omega(\xi,q(\xi))=0. \tag{33}$$

After simplification, Equation (33) will be

$$D^6q(\xi)+\frac{2\eta}{\xi}D^5q(\xi)+\frac{\eta(\eta-1)}{\xi^2}D^4q(\xi)+\omega(\xi,q(\xi))=0. \tag{34}$$

The Equation (34) in fractional order is taken as

$$D^{6\sigma}q(\xi)+\frac{2\eta}{\xi^{\sigma}}D^{5\sigma}q(\xi)+\frac{\eta(\eta-1)}{\xi^{2\sigma}}D^{4\sigma}q(\xi)+\omega(\xi,q(\xi))=0. \tag{35}$$

with initial conditions $q(0)=\phi_0, q^{(\sigma)}(0)=\phi_1, q^{(2\sigma)}(0)=\phi_2, q^{(3\sigma)}(0)=\phi_3, q^{(4\sigma)}(0)=\phi_4$, $q^{(5\sigma)}(0)=\phi_5$, where $q^{(\sigma)}, q^{(2\sigma)}, q^{(3\sigma)}, q^{(4\sigma)}, q^{(5\sigma)}$ denotes the Caputo derivative of order σ, 2σ, 3σ, 4σ, 5σ, respectively.

Case 5: When $\beta=1$, $\gamma=5$, the equation will be

$$\xi^{-\eta}D^1\left(\xi^{\eta}D^5\right)q+\omega(\xi,q(\xi))=0. \tag{36}$$

After simplification, Equation (36) will be

$$D^6q(\xi)+\frac{\eta}{\xi}D^5q(\xi)+\omega(\xi,q(\xi))=0. \tag{37}$$

The Equation (37) in fractional order is taken as

$$D^{6\sigma}q(\xi)+\frac{\eta}{\xi^{\sigma}}D^{5\sigma}q(\xi)+\omega(\xi,q(\xi))=0. \tag{38}$$

with initial conditions $q(0) = \phi_0, q^{(\sigma)}(0) = \phi_1, q^{(2\sigma)}(0) = \phi_2, q^{(3\sigma)}(0) = \phi_3, q^{(4\sigma)}(0) = \phi_4,$ $q^{(5\sigma)}(0) = \phi_5$, where $q^{(\sigma)}, q^{(2\sigma)}, q^{(3\sigma)}, q^{(4\sigma)}, q^{(5\sigma)}$ denotes the Caputo derivative of order σ, $2\sigma, 3\sigma, 4\sigma, 5\sigma$, respectively.

4. Method

Consider the general Equation (1)

$$\xi^{-\eta} D^{\beta}(\xi^{\eta} D^{\gamma})q = \omega(\xi, q(\xi)).$$

After simplifying and expanding this equation, we have

$$\begin{aligned} &D^{\beta+\gamma}q(\xi)+{}^{\beta}C_{\beta-1}\left(\frac{\eta}{\xi}\right)D^{\beta+\gamma-1}q(\xi)+{}^{\beta}C_{\beta-2}\left(\frac{\eta(\eta-1)}{\xi^2}\right)D^{\beta+\gamma-2}q(\xi)+\dots \\ &{}^{\beta}C_0\left(\frac{\eta(\eta-1)(\eta-2)(\eta-3)\dots(\eta-\beta+1)}{\xi^{\beta}}\right)D^{\gamma}q(\xi)+\omega(\xi,q(\xi))=0. \end{aligned} \tag{39}$$

we generalize this Equation (39) into fractional form as

$$\begin{aligned} &D_{\xi}^{(\beta+\gamma)\sigma}q(\xi)+{}^{\beta}C_{\beta-1}\left(\frac{\eta}{\xi^{\sigma}}\right)D_{\xi}^{(\beta+\gamma-1)\sigma}q(\xi)+{}^{\beta}C_{\beta-2}\left(\frac{\eta(\eta-1)}{\xi^{2\sigma}}\right)D_{\xi}^{(\beta+\gamma-2)\sigma}q(\xi)+\dots \\ &{}^{\beta}C_0\left(\frac{\eta(\eta-1)(\eta-2)(\eta-3)\dots(\eta-\beta+1)}{\xi^{\beta\sigma}}\right)D_{\xi}^{(\gamma)\sigma}q(\xi)+\omega(\xi,q(\xi))=0, \end{aligned} \tag{40}$$

with initial conditions $q(0) = \phi_0, q^{(\sigma)}(0) = \phi_1, q^{(2\sigma)}(0) = \phi_2, \dots q^{((\beta+\gamma-1)\sigma)}(0) = \phi_{\beta+\gamma-1}$, where $q^{(\sigma)}, q^{(2\sigma)}$ denotes the caputo derivative of order σ and 2σ . $D_{\xi} = \frac{d}{d\xi}$ in (40) represents Caputo fractional differential operator.

Clearly, when $\beta = 1$, $\gamma = 1$ and $\eta = 2$, we have the Equation (63) in example 7. In a similar fashion, we can extract all the examples by applying different values of β, γ, η.

Now, we discuss the method.

- ***Step 1*:** We approximate the highest-order derivative using Haar functions:

$$D_{\xi}^{(\beta+\gamma)\sigma}q(\xi) = \sum_{\tau=1}^{2L} \lambda_{\tau} h_{\tau}. \tag{41}$$

- ***Step 2*:** We integrate the Equation (41) again and again, and after applying the initial conditions, we get

$$D_{\xi}^{(\beta+\gamma-1)\sigma}q(\xi) = \phi_{\beta+\gamma-1} + \sum_{\tau=1}^{2L} \lambda_{\tau}\rho_{\tau,\sigma}(\xi), \tag{42}$$

$$D_{\xi}^{(\beta+\gamma-2)\sigma}q(\xi) = \phi_{\beta+\gamma-2} + \frac{\xi^{\sigma}}{\Gamma(\sigma+1)}\phi_{\beta+\gamma-1} + \sum_{\tau=1}^{2L} \lambda_{\tau}\rho_{\tau,2\sigma}(\xi).$$

and so on. The last term is

$$q(\xi) = \sum_{\tau=1}^{2L} \lambda_{\tau}\rho_{\tau,(\beta+\gamma)\sigma}(\xi) + \frac{\xi^{(\beta+\gamma-1)\sigma}}{\Gamma((\beta+\gamma-1)\sigma+1)}\phi_{\beta+\gamma-1} + \dots \phi_0. \tag{43}$$

- ***Step 3*:** We collocate the points as

$$\xi_{\tau} = \frac{\tau - 0.5}{2L}, \tau = 1, 2, \dots 2L.$$

Now, we substitute all the values of derivatives into Equation (40) and collocate the points, resulting in the system of differential equations as follows

$$\begin{aligned}&\sum_{\tau=1}^{2L} \lambda_\tau h_\tau(\xi_\tau) + {}^{\beta}C_{\beta-1}\left(\frac{\eta}{\xi_\tau{}^\sigma}\right)\left(\phi_{\beta+\gamma-1} + \sum_{\tau=1}^{2L} \lambda_\tau \rho_{\tau,\sigma}(\xi_\tau)\right) + \dots \\ &\omega(\xi_\tau, \sum_{\tau=1}^{2L} \lambda_\tau \rho_{\tau,(\beta+\gamma)\sigma}(\xi_\tau) + \frac{\xi_\tau{}^{(\beta+\gamma-1)\sigma}}{\Gamma((\beta+\gamma-1)\sigma+1)}\phi_{\beta+\gamma-1} + \dots \phi_0) = 0.\end{aligned} \tag{44}$$

- ***Step 4*:** We solve the system of equations (44) using the Newton method and obtain the values of the Haar coefficients $\lambda_\tau, \tau = 1, 2, \dots 2L$.
- ***Step 5*:** After substituting the values of Haar coefficients into Equation (43), we obtain the numerical solution of Equation (40).

5. Convergence Analysis

Lemma 1 ([34]). *Assume that $q(\xi) \in L_2(\Re)$ and has a bounded first derivative, that is, $|q'(\xi)| \le G$, $\forall \xi \in (0,1), P > 0$ and $q(\xi) = \sum_{\tau=1}^{\infty} \lambda_\tau h_\tau(\xi)$. Then, $|\lambda_j| \le G2^{-(3l-2)/2}$.*

Theorem 1 ([34]). *Suppose $q(\xi) \in L_2(\Re)$ is a continuous function with a bounded first derivative in (0,1). Then, the error norm at the Jth level satisfies*

$$||E_J|| \le \sqrt{\frac{G}{12}} D 2^{-(3/2)L}$$

where $|q'(\xi)| \le G, \forall \xi \in (0,1)$, $G > 0$ and $M = 2^J$, where J is maximum resolution.

Proof. The proof is straightforward. We can refer to [34]. □

5.1. Numerical Error

The maximum absolute error is given by

$$E_C = Max.|q_\tau^{exact} - q_\tau^{approx.}|,$$

where q_τ^{exact} and $q_\tau^{approx.}$ are exact and approximate solutions at the τth collocation point.

5.2. Rate of Convergence

Rate of convergence is defined by

$$R_C(L) = \frac{\log[E_C(L/2)/E_C(L)]}{\log 2},$$

where $E_C(L)$ represents the maximum absolute error at L collocation points.

5.3. Stability

The condition number is significant to measure the stability of an algorithm[35]. For stability, the condition number should be bounded. We consider the system of equations formed in our algorithm as

$$\mathrm{HA} = \mathrm{Y},$$

where H denotes the Haar weights, A denotes the unknown Haar coefficients and Y is a known vector. The condition number bound for some examples is given in Table 1.

Definition 3 ([36]). *Let us consider the system of equations to be of type* HA = Y, *if the inverse of* H *exists and is bounded, then the algorithm is stable; that is,*

$$||\mathrm{H}^{-1}|| \le \mathrm{Z},$$

where Z is a constant.

The Condition number is bounded [35]; that is,

$$Cond(\mathrm{H})_2 \leq ||\mathrm{H}||^2||\mathrm{H}^{-1}||^2.$$

Table 1. Condition number bound for Examples 1 and 3.

Resolution	Size	Example 1	Example 3
3	16×16	1.4133×10^2	1.8795×10^2
4	32×32	2.8277×10^2	3.8086×10^2
5	64×64	5.6547×10^2	7.6413×10^2

6. Applications

Example 1. *Taking $\eta = 2$ in Equation (8) gives us this fourth-order fractional Lane-Emden-Fowler equation:*

$$D_{\xi}^{4\sigma}q(\xi) + \frac{4}{\xi^{\sigma}}D_{\xi}^{3\sigma}q(\xi) + \frac{2}{\xi^{2\sigma}}D_{\xi}^{2\sigma}q(\xi) = 3(12 - 53\xi^4 + 12\xi^8)(q(\xi))^{-15}, \tag{45}$$

with initial conditions $q(0) = 1, q^{(\sigma)}(0) = 0, q^{(2\sigma)}(0) = 0, q^{(3\sigma)}(0) = 0.$

Now, we apply the method, and using initial conditions, we can write

$$q(\xi) = 1 + \sum_{\tau=1}^{2L} \lambda_{\tau}\rho_{\tau,4\sigma}(\xi). \tag{46}$$

After substituting all the values of $q(\xi)$ and its derivatives into (45) and using collocation of points, we obtain a system of nonlinear equations as follows:

$$\begin{aligned} &\sum_{\tau=1}^{2L} \lambda_{\tau}h_{\tau}(\xi_{\tau}) + \tfrac{4}{\xi_{\tau}^{\sigma}}\sum_{\tau=1}^{2L} \lambda_{\tau}\rho_{\tau,\sigma}(\xi_{\tau}) + \tfrac{2}{\xi_{\tau}^{2\sigma}}\sum_{\tau=1}^{2L} \lambda_{\tau}\rho_{\tau,2\sigma}(\xi_{\tau}) \\ &-3(12 - 53\xi_{\tau}^4 + 12\xi_{\tau}^8)(1 + \sum_{\tau=1}^{2L} \lambda_{\tau}\rho_{\tau,4\sigma}(\xi_{\tau}))^{-15} = 0. \end{aligned} \tag{47}$$

We can easily solve this system (47) using the Newton method. After solving this system, we have the values of the Haar coefficients $\lambda_{\tau}, \tau = 1, 2, \ldots 2L$ and substituting these values into (46) gives the approximate solution.

The exact solution of (45) when $\sigma = 1$ is $q(\xi) = (1 + \xi^4)^{\frac{1}{4}}$. which is given in [37].

Example 2. *When we substitute $\eta = 2$ in Equation (11), we get this fourth-order fractional Lane-Emden-Fowler equation:*

$$D_{\xi}^{4\sigma}q(\xi) + \frac{2}{\xi^{\sigma}}D_{\xi}^{3\sigma}q(\xi) + \xi(q(\xi))^{-2} = \omega(\xi), \tag{48}$$

with initial conditions $q(0) = 0, q^{(\sigma)}(0) = 0, q^{(2\sigma)}(0) = 0, q^{(3\sigma)}(0) = 0$, where

$$\omega(\xi) = \Gamma(1 + 4\sigma) + 8\frac{\Gamma(4\sigma)}{\Gamma(\sigma)} + \xi\left(1 + \xi^{4\sigma}\right)^{-2}$$

Now, we apply the method, and using the initial conditions, we can write

$$q(\xi) = 1 + \sum_{\tau=1}^{2L} \lambda_{\tau}\rho_{\tau,4\sigma}(\xi). \tag{49}$$

After substituting all the values of $q(\xi)$ and its derivatives into (48) and using collocation of points, we get a system of nonlinear equations as follows:

$$\sum_{\tau=1}^{2L}\lambda_\tau h_\tau(\xi_\tau)+\frac{2}{\xi_\tau^\sigma}\sum_{\tau=1}^{2L}\lambda_\tau\rho_{\tau,\sigma}(\xi_\tau)+\xi_\tau(1+\sum_{\tau=1}^{2L}\lambda_\tau\rho_{\tau,4\sigma}(\xi_\tau))^{-2}-\omega(\xi_\tau)=0. \quad (50)$$

We can easily solve this system (50) using the Newton method. After solving this system, we have the values of the Haar coefficients $\lambda_\tau, \tau = 1, 2, \ldots 2L$, and these values in (49) give the approximate solution.

The exact solution of (48) is $q(\xi) = 1 + \xi^4$, when $\sigma = 1$.

Example 3. *Taking $\eta = 4$ in Equation (14) gives the fifth-order fractional Lane-Emden-Fowler equation:*

$$\begin{aligned}&D_\xi^{5\sigma}q(\xi)+\tfrac{16}{\xi^\sigma}D_\xi^{4\sigma}q(\xi)+\tfrac{72}{\xi^{2\sigma}}D_\xi^{3\sigma}q(\xi)\\&+\tfrac{96}{\xi^{3\sigma}}D_\xi^{2\sigma}q(\xi)+\tfrac{24}{\xi^{4\sigma}}D_\xi^{\sigma}q(\xi)+(1-\xi^{5\sigma})(q(\xi))+\xi^{10\sigma}=\omega(\xi),\end{aligned} \quad (51)$$

with initial conditions $q(0) = 0, q^{(\sigma)}(0) = 0, q^{(2\sigma)}(0) = 0, q^{(3\sigma)}(0) = 0, q^{(4\sigma)}(0) = 0$, where

$$\omega(\xi)=1+\Gamma(1+5\sigma)+80\frac{\Gamma(5\sigma)}{\Gamma(\sigma)}+180\frac{\Gamma(5\sigma)}{\Gamma(2\sigma)}+160\frac{\Gamma(5\sigma)}{\Gamma(3\sigma)}+30\frac{\Gamma(5\sigma)}{\Gamma(4\sigma)}$$

Now, we apply the method, and using initial conditions, we can write

$$q(\xi)=1+\sum_{\tau=1}^{2L}\lambda_\tau\rho_{\tau,5\sigma}(\xi). \quad (52)$$

After putting all the values of $q(\xi)$ and its derivatives into (51) we get a system of nonlinear equations as:

$$\begin{aligned}&\sum_{\tau=1}^{2L}\lambda_\tau h_\tau(\xi_\tau)+\tfrac{16}{\xi_\tau^\sigma}\sum_{\tau=1}^{2L}\lambda_\tau\rho_{\tau,\sigma}(\xi_\tau)+\tfrac{72}{\xi_\tau^{2\sigma}}\sum_{\tau=1}^{2L}\lambda_\tau\rho_{\tau,2\sigma}(\xi_\tau)+\tfrac{96}{\xi_\tau^{3\sigma}}\sum_{\tau=1}^{2L}\lambda_\tau\rho_{\tau,3\sigma}(\xi_\tau)\\&+\tfrac{24}{\xi_\tau^{4\sigma}}\sum_{\tau=1}^{2L}\lambda_\tau\rho_{\tau,4\sigma}(\xi_\tau)+(1-\xi_\tau^{5\sigma})(1+\sum_{\tau=1}^{2L}\lambda_\tau\rho_{\tau,5\sigma}(\xi_\tau))+\xi_\tau^{10\sigma}-\omega(\xi_\tau)=0.\end{aligned} \quad (53)$$

We can easily solve this system (53) using the Newton method. After solving this system, we have the values of Haar coefficients $\lambda_\tau, \tau = 1, 2, \ldots 2L$ and putting these values in (52) gives the approximate solution.

The exact solution of (51) is $q(\xi) = 1 + \xi^{5\sigma}$.

Example 4. *When we put $\eta = 4$ in Equation (32) we get this sixth-order fractional Lane-Emden-Fowler equation:*

$$\begin{aligned}&D_\xi^{6\sigma}q(\xi)+\tfrac{12}{\xi^\sigma}D_\xi^{5\sigma}q(\xi)+\tfrac{36}{\xi^{2\sigma}}D_\xi^{4\sigma}q(\xi)+\tfrac{24}{\xi^{3\sigma}}D_\xi^{3\sigma}q(\xi)\\&-45(-280+17056\xi^6-79987\xi^{12}+63332\xi^{18}-7712\xi^{24}+32\xi^{30})(q(\xi))^{13}=0,\end{aligned} \quad (54)$$

with initial conditions $q(0) = 1, q^{(\sigma)}(0) = 0, q^{(2\sigma)}(0) = 0, q^{(3\sigma)}(0) = 0, q^{(4\sigma)}(0) = 0, q^{(5\sigma)}(0) = 0$.

Now, we apply the method, and using the initial conditions, we can write

$$q(\xi)=1+\sum_{\tau=1}^{2L}\lambda_\tau\rho_{\tau,6\sigma}(\xi). \quad (55)$$

After putting all the values of $q(\xi)$ and its derivatives into (54), we get a system of nonlinear equations as follows:

$$\begin{aligned}&\sum_{\tau=1}^{2L}\lambda_\tau h_\tau(\xi_\tau)+\tfrac{12}{\xi_\tau^{\sigma}}\sum_{\tau=1}^{2L}\lambda_\tau\rho_{\tau,\sigma}(\xi_\tau)+\tfrac{36}{\xi_\tau^{2\sigma}}\sum_{\tau=1}^{2L}\lambda_\tau\rho_{\tau,2\sigma}(\xi_\tau)+\tfrac{24}{\xi_\tau^{3\sigma}}\sum_{\tau=1}^{2L}\lambda_\tau\rho_{\tau,3\sigma}(\xi_\tau)\\&-45(-280+17056\xi_\tau^6-79987\xi_\tau^{12}+63332\xi_\tau^{18}-7712\xi_\tau^{24}+32\xi_\tau^{30})(1+\sum_{\tau=1}^{2L}\lambda_\tau\rho_{\tau,6\sigma}(\xi_\tau))^{13}=0.\end{aligned}\tag{56}$$

We can easily solve this system (53) *using the Newton method. After solving this system, we have the values of Haar coefficients* $\lambda_\tau, \tau = 1, 2, \ldots 2L$ *and substituting these values into* (52) *gives the approximate solution.*

The exact solution of (54) *when* $\sigma = 1$ *is* $q(\xi) = \frac{1}{\sqrt{1+\xi^6}}$.

Example 5. *Consider the fractional Lane-Emden Fowler equation, [38]:*

$$D_\xi^{2\sigma}q(\xi)+\frac{1}{\xi^\sigma}D_\xi^{\sigma}q(\xi)+(1+\xi^\sigma)(q(\xi))^5=\omega(\xi),\tag{57}$$

with initial conditions $q(0) = 3, q^{(\sigma)}(0) = 0$*, where*

$$\omega(\xi)=\Gamma(1+2\sigma)+\frac{\Gamma(1+2\sigma)}{\Gamma(1+\sigma)}+(1+\xi^\sigma)\left(3+\xi^{2\sigma}\right)^5.$$

The exact solution of (57) *is* $q(\xi) = \left(3 + \xi^{2\sigma}\right)$.

Now, we apply the method, and using the initial conditions, we can write

$$q(\xi)=3+\sum_{\tau=1}^{2L}\lambda_\tau\rho_{\tau,2\sigma}(\xi).\tag{58}$$

After putting all the values of $q(\xi)$ *and its derivatives into* (57)*, we get a system of nonlinear equations as follows:*

$$\begin{aligned}&\sum_{\tau=1}^{2L}\lambda_\tau h_\tau(\xi_\tau)+\tfrac{1}{\xi_\tau^{\sigma}}\sum_{\tau=1}^{2L}\lambda_\tau\rho_{\tau,\sigma}(\xi_\tau)+(1+\xi_\tau^\sigma)(3+\sum_{\tau=1}^{2L}\lambda_\tau\rho_{\tau,2\sigma}(\xi_\tau))^5\\&-\Gamma(1+2\sigma)-\tfrac{\Gamma(1+2\sigma)}{\Gamma(1+\sigma)}-(1+\xi_\tau^\sigma)\left(3+\xi_\tau^{2\sigma}\right)^5=0.\end{aligned}\tag{59}$$

We can easily solve this system (59) *using the Newton method. After solving this system, we have the values of Haar coefficients* $\lambda_\tau, \tau = 1, 2, \ldots 2L$ *and putting these values in* (58) *gives the approximate solution.*

Example 6. *Consider this third-order fractional Lane-Emden-Fowler equation:*

$$D_\xi^{3\sigma}q(\xi)+\frac{3}{\xi^\sigma}D_\xi^{2\sigma}q(\xi)-(q(\xi))^3=\omega(\xi),\tag{60}$$

with initial conditions $q(0) = 0, q^{(\sigma)}(0) = 0, q^{(2\sigma)}(0) = 0$*, where*

$$\begin{aligned}\omega(\xi)=&-\xi^{9\sigma}e^\xi+\xi^{3\sigma}e^\xi+9\sigma^2\xi^{3\sigma-1}e^\xi+\tfrac{(3\sigma)^2(3\sigma-1)^2}{2}\xi^{3\sigma-2}e^\xi\\&+3\xi^{2\sigma}e^\xi+18\sigma^2\xi^{2\sigma-1}e^\xi+9\sigma^2(3\sigma-1)(2\sigma-1)\xi^{2\sigma-2}e^\xi\\&+\tfrac{(3\sigma)^2(3\sigma-1)^2(3\sigma-2)^2}{6}e^\xi.\end{aligned}$$

Clearly, when $\sigma = 1$*, Equation* (60) *becomes*

$$q'''(\xi)+\frac{3}{\xi}q''(\xi)-(q(\xi))^3=24e^\xi+36\xi e^\xi+12\xi^2e^\xi+\xi^3e^\xi-\xi^9e^{3\xi},$$

which is given in [39].

Now, we apply the method, and using the initial conditions, we can write

$$q(\xi) = \sum_{\tau=1}^{2L} \lambda_\tau \rho_{\tau,3\sigma}(\xi). \tag{61}$$

After putting all the values of $q(\xi)$ and its derivatives into (60), we get a system of nonlinear equations as follows:

$$\sum_{\tau=1}^{2L} \lambda_\tau h_\tau(\xi_\tau) + \frac{3}{\xi_\tau^\sigma} \sum_{\tau=1}^{2L} \lambda_\tau \rho_{\tau,\sigma}(\xi_\tau) - (\sum_{\tau=1}^{2L} \lambda_\tau \rho_{\tau,3\sigma}(\xi_\tau))^3 - \omega(\xi_\tau) = 0. \tag{62}$$

We can easily solve this system (62) using the Newton method. After solving this system, we have the values of Haar coefficients $\lambda_\tau, \tau = 1, 2, \ldots 2L$ and substituting these values into (61) gives the approximate solution.

The exact solution of (60) is $q(\xi) = \xi^{3\sigma} e^{\xi}$.

Example 7. *Consider the fractional Lane-Emden-Fowler equation, which is given in [40]*

$$D_\xi^{2\sigma} q(\xi) + \frac{2}{\xi^\sigma} D_\xi^\sigma q(\xi) + 8e^{q(\xi)} + 4e^{q(\xi)/2} = 0, \tag{63}$$

with initial conditions $q(0) = 0, q^{(\sigma)}(0) = 0$. The exact solution of (63) when $\sigma = 1$ is $q(\xi) = -2\log(1 + \xi^2)$.

Now, we apply the method

$$D_\xi^{2\sigma} q(\xi) = \sum_{\tau=1}^{2L} \lambda_\tau h_\tau. \tag{64}$$

Integrating (64) and applying the initial condition gives us

$$D_\xi^\sigma q(\xi) = \sum_{\tau=1}^{2L} \lambda_\tau \rho_{\tau,\sigma}(\xi).$$

In the same way, we can write

$$q(\xi) = \sum_{\tau=1}^{2L} \lambda_\tau \rho_{\tau,2\sigma}(\xi). \tag{65}$$

After substituting all the values of $q(\xi)$ and its derivatives into (63) and after collocation of points, we get a system of nonlinear equations as follows:

$$\sum_{\tau=1}^{2L} \lambda_\tau h_\tau(\xi_\tau) + \frac{2}{\xi^\sigma} \sum_{\tau=1}^{2L} \lambda_\tau \rho_{\tau,\sigma}(\xi_\tau) + 8e^{\sum_{\tau=1}^{2L} \lambda_\tau \rho_{\tau,2\sigma}(\xi_\tau)} + 4e^{\frac{\left(\sum_{\tau=1}^{2L} \lambda_\tau \rho_{\tau,2\sigma}(\xi_\tau)\right)}{2}} = 0. \tag{66}$$

Using the Newton method, we can easily solve this system (66). After solving this system, we have the values of the Haar coefficients $\lambda_\tau, \tau = 1, 2, \ldots 2L$ and putting these values in (65) gives the approximate solution.

7. Numerical Simulation and Conclusions

This paper uses the Haar wavelet collocation method to find the numerical solution to the general-order fractional Lane-Emden-Fowler equation. This numerical scheme is presented in general order. We have documented many examples of second-, third-, fourth-, fifth-, and sixth-order fractional differential equations. We have numerically simulated those examples graphically and in tabular format. It is clear from the simulations that this method works very nicely. Figures 1 and 2 show the comparison of exact and numerical solutions and the absolute error of Example 1 for $\sigma = 1$ respectively. Figures 3 and 4 show the HWCM solution for different values of σ and Haar coefficients of Example 1 respectively. Figures 5 and 6 show the comparison of exact and numerical solutions and the absolute error of Example 2 for $\sigma = 1$ respectively. Figures 7 and 8 show the HWCM solution for different values of σ and Haar coefficients respectively. Figures 9 and 10 show the comparison of exact and numerical solutions and the absolute error of Example 3 for $\sigma = 1$ respectively. Figures 11 and 12 show the HWCM solution for different values of σ and Haar coefficients respectively. Similarly, Figures 13 and 14 show the comparison of exact and numerical solutions and the absolute error of Example 4 for $\sigma = 1$ respectively. Figures 15 and 16 show the HWCM solution for different values of σ and Haar coefficients respectively. Figures 17 and 18 show the comparison of exact and numerical solutions and the absolute error of Example 5 for $\sigma = 1$ respectively. Figures 19 and 20 show the HWCM solution for different values of σ and Haar coefficients respectively. Figures 21 and 22 show the comparison of exact and numerical solutions and the absolute error of Example 6 for $\sigma = 1$ respectively. Figures 23 and 24 show the HWCM solution for different values of σ and Haar coefficients respectively. Figures 25 and 26 show the comparison of exact and numerical solutions and the absolute error of Example 7 for $\sigma = 1$ respectively. Figures 27 and 28 show the HWCM solution for different values of σ and Haar coefficients respectively. Tables 2–15 give us a comparison of the numerical values of Haar and the exact solution and document the numerical values for different values of σ. From all the tables and graphs, we conclude that the method is quite accurate and gives us good outcomes.

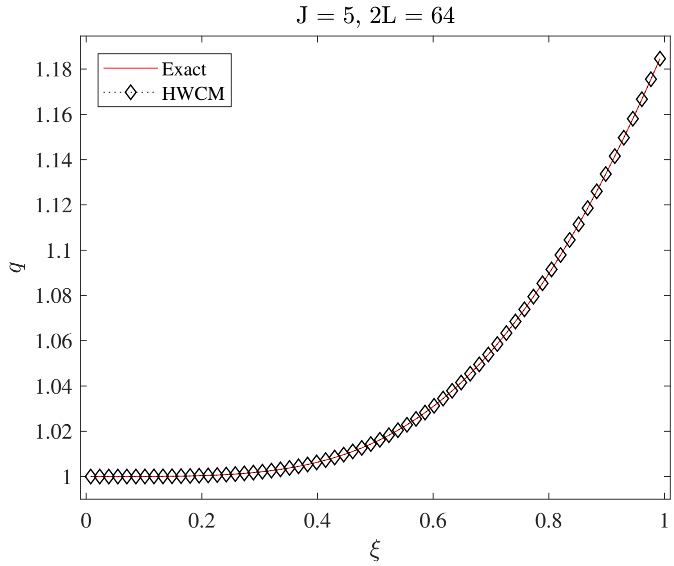

Figure 1. Comparison of Exact and HWCM solution of Example 1 when $\sigma = 1$.

Table 2. Comparison of HWCM and exact solution of Example 1 for J = 5.

ξ	HWCM	Exact	ψ_{10} [37]	QBSM [37]	ψ_8 [37]	$\sigma = 0.75$	$\sigma = 0.85$	$\sigma = 0.95$
0.1	1.00002	1.00002	1.00003	1.00003	1.00003	1.00087	1.00021	1.00005
0.4	1.00633	1.00633	1.00634	1.00634	1.00634	1.04867	1.02305	1.00989
0.5	1.01527	1.01527	1.01527	1.01527	1.01527	1.08507	1.04683	1.02262
0.6	1.03093	1.03093	1.03093	1.03093	1.03093	1.12870	1.08112	1.04374
0.9	1.13442	1.13441	1.13440	1.13438	1.13438	1.27334	1.23519	1.16789

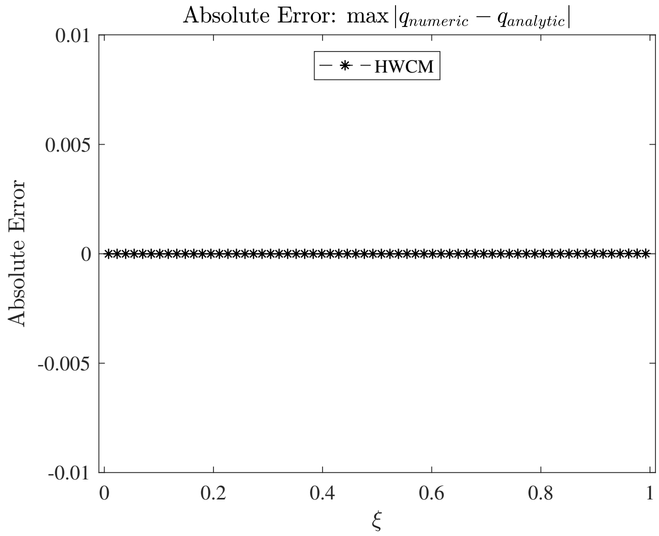

Figure 2. Absolute error of HWCM of Example 1 when σ = 1.

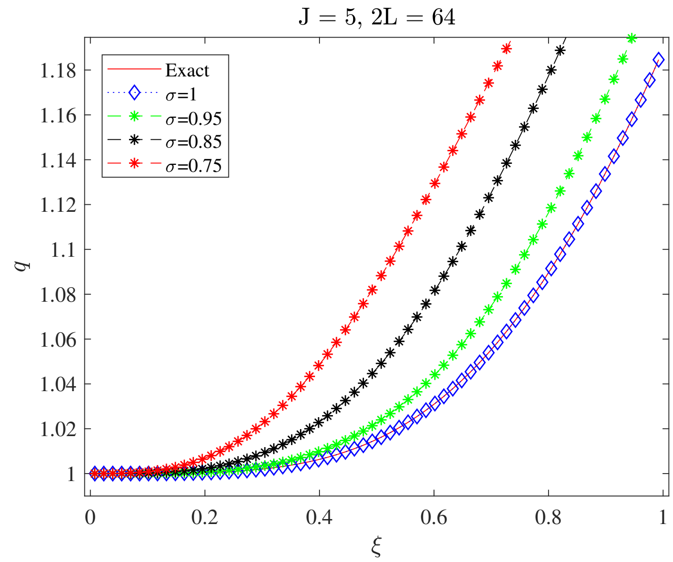

Figure 3. HWCM solution of Example 1 for different values of σ.

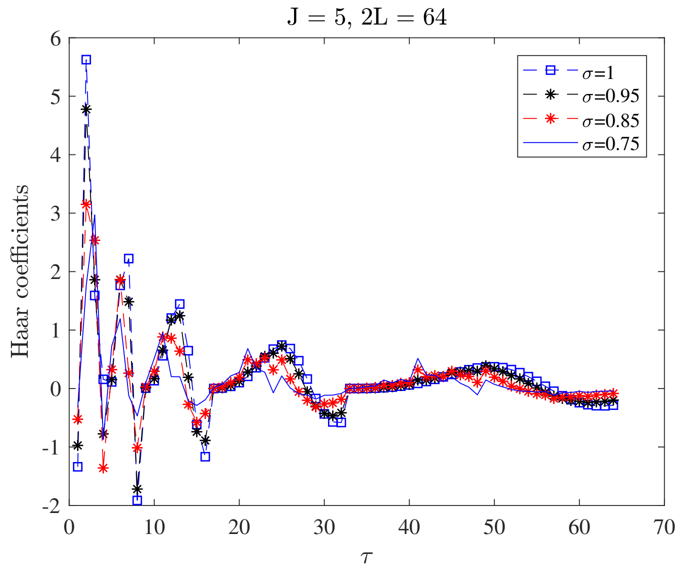

Figure 4. Haar coefficients of Example 1 for different values of σ.

Table 3. Error Comparison of Example 1.

ξ	**HWCM Error**	E_8 [37]	E_{10} [37]
0.1	0	6.6342×10^{-6}	2.1208×10^{-6}
0.4	3.1×10^{-8}	4.0829×10^{-6}	1.3122×10^{-6}
0.5	2.01×10^{-7}	6.8710×10^{-7}	2.2781×10^{-7}
0.6	4.19×10^{-7}	4.7993×10^{-6}	1.5386×10^{-6}
0.9	5.85×10^{-6}	3.4277×10^{-5}	1.1079×10^{-5}

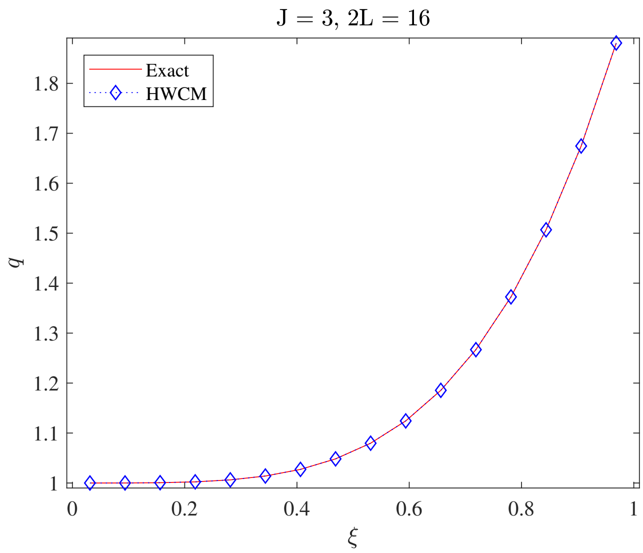

Figure 5. Comparison of Exact and HWCM solution of Example 2 when $\sigma = 1$.

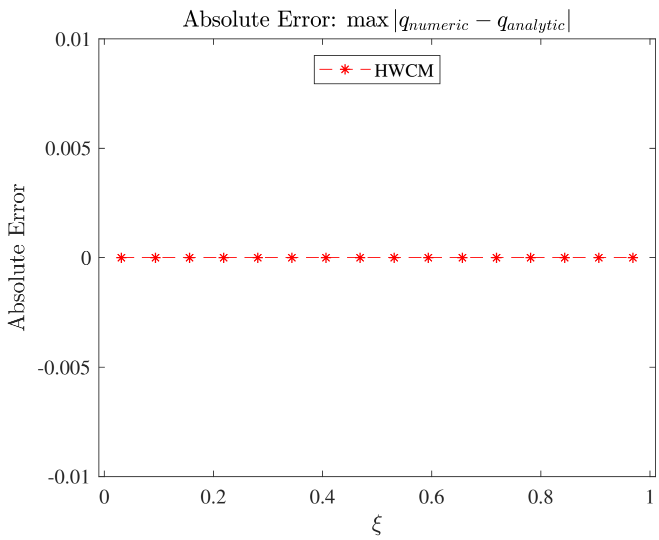

Figure 6. Absolute error of HWCM of Example 2 when σ = 1.

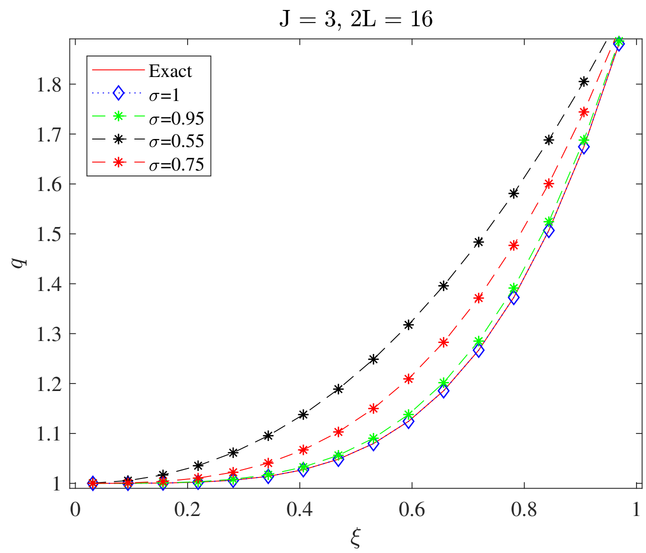

Figure 7. HWCM solution of Example 2 for different values of σ.

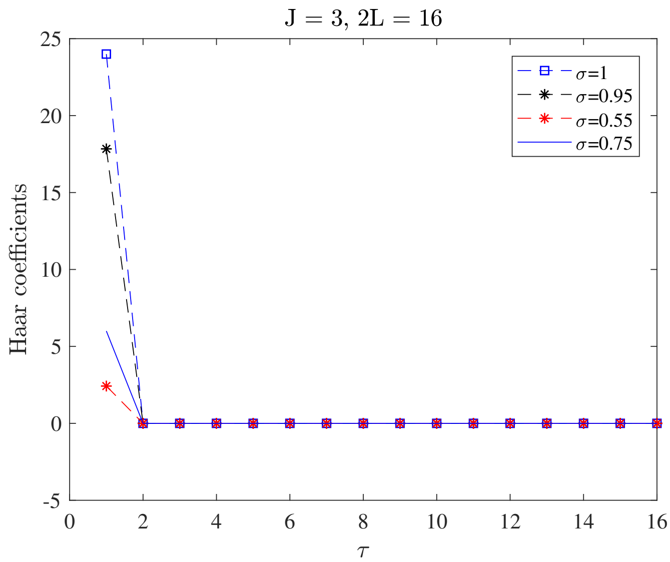

Figure 8. Haar coefficients of Example 2 for different values of σ.

Table 4. Comparison of HWCM and exact solution of Example 2 for J = 3.

$\xi/32$	Haar Solution	Exact Solution	$\sigma = 0.55$	$\sigma = 0.75$	$\sigma = 0.95$
1/32	1.00000095	1.00000095	1.00048828	1.00003052	1.00000191
3/32	1.00007725	1.00007725	1.0054744	1.00082397	1.00012402
5/32	1.00059605	1.00059605	1.0168424	1.0038147	1.000864
7/32	1.00228977	1.00228977	1.03530903	1.01046753	1.00310315
9/32	1.00625706	1.00625706	1.0613767	1.02224731	1.00806402
11/32	1.01396275	1.01396275	1.09544077	1.0406189	1.01728711
13/32	1.02723789	1.02723789	1.13783053	1.06704712	1.03261481
15/32	1.04827976	1.04827976	1.18882992	1.10299683	1.05617937
17/32	1.07965183	1.07965183	1.24868963	1.14993286	1.09039325
19/32	1.12428379	1.12428379	1.31763472	1.20932007	1.13794113
21/32	1.18547153	1.18547153	1.39586991	1.28262329	1.20177316
23/32	1.26687717	1.26687717	1.48358329	1.37130737	1.28509911
25/32	1.37252903	1.37252903	1.58094908	1.47683716	1.39138314
27/32	1.50682163	1.50682163	1.68812974	1.60067749	1.52433927
29/32	1.67451572	1.67451572	1.80527765	1.74429321	1.68792719
31/32	1.88073826	1.88073826	1.93253636	1.90914917	1.88634851

Table 5. Absolute error of HWCM of Example 2 for $\sigma = 1$.

Resolution (J)	**3**	**4**	**5**	**6**	**7**	**8**
HWM error	2.2204×10^{-16}	0	0	4.4409×10^{-16}	0	0
CPU time (seconds)	1.132563	1.383034	1.861307	4.541592	18.758987	125.318744

Table 6. Absolute error of HWCM of Example 2 for different σ.

Resolution	**3**	**4**	**5**	**6**	**7**
$\sigma = 0.55$	3.4658×10^{-11}	3.7683×10^{-11}	3.9526×10^{-11}	4.0468×10^{-11}	4.0935×10^{-11}
$\sigma = 0.75$	1.207×10^{-12}	1.3634×10^{-16}	1.4571×10^{-16}	1.5068×10^{-16}	1.533×10^{-16}
$\sigma = 0.95$	2.2204×10^{-16}	4.4409×10^{-16}	4.4409×10^{-16}	2.2204×10^{-16}	2.2204×10^{-16}

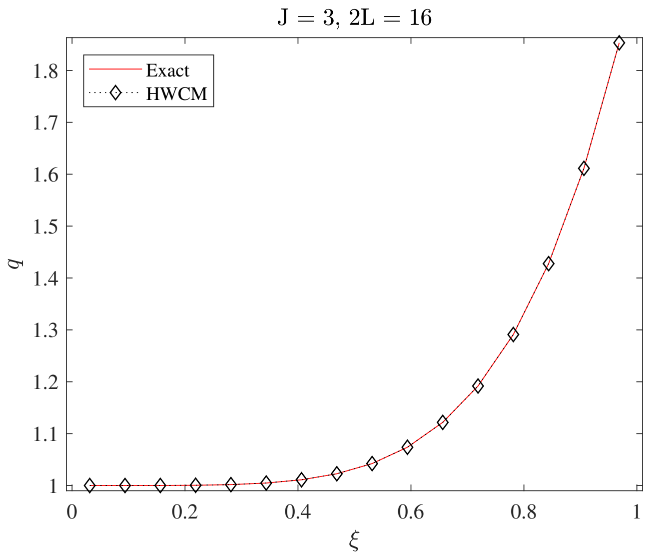

Figure 9. Comparison of Exact and HWCM solution of Example 3 when $\sigma = 1$.

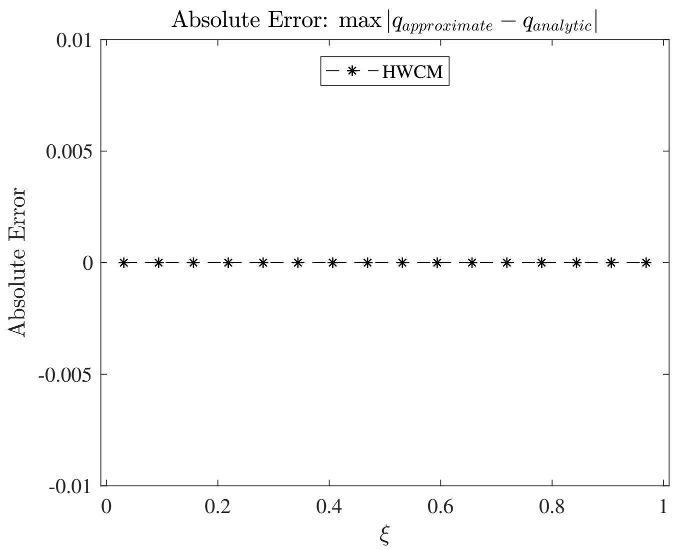

Figure 10. Absolute error of HWCM of Example 3 when σ = 1.

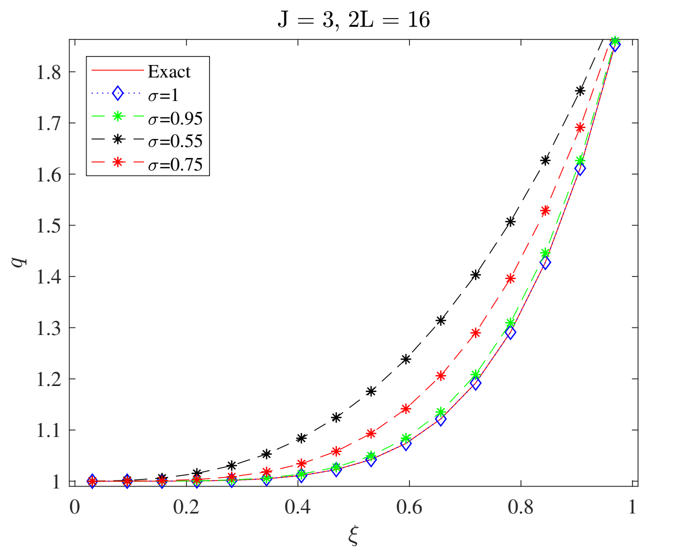

Figure 11. HWCM solution of Example 3 for different values of σ.

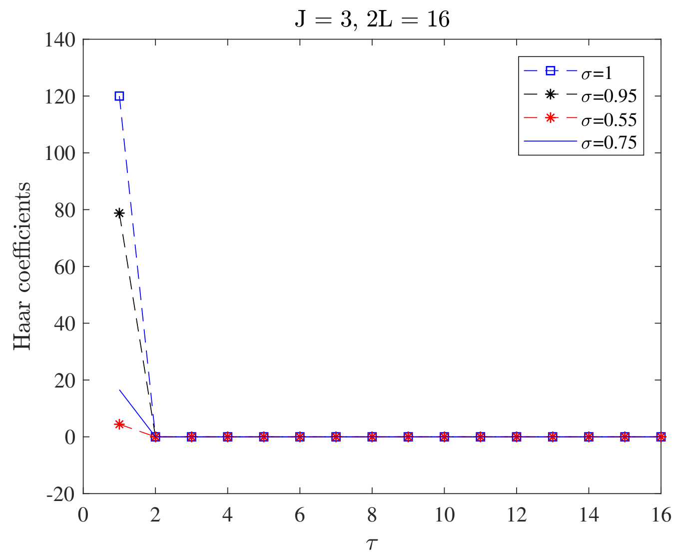

Figure 12. Haar coefficients of Example 3 for different values of σ.

Table 7. Comparison of HWCM and exact solution of Example 3 for J = 3.

$\xi/32$	Haar Solution	Exact Solution	$\sigma = 0.55$	$\sigma = 0.75$	$\sigma = 0.95$
1/32	1.00000003	1.00000003	1.00007258	1.00000227	1.00000007
3/32	1.00000724	1.00000724	1.00148909	1.0001396	1.00001309
5/32	1.00009313	1.00009313	1.00606743	1.00094804	1.00014813
7/32	1.00050089	1.00050089	1.01530582	1.00334815	1.00073241
9/32	1.0017598	1.0017598	1.03054949	1.00859205	1.00241652
11/32	1.00479969	1.00479969	1.05304775	1.01823518	1.00626834
13/32	1.01106539	1.01106539	1.08398105	1.03411733	1.01386017
15/32	1.02263114	1.02263114	1.1244767	1.0583485	1.02735087
17/32	1.04231504	1.04231504	1.17561905	1.0932977	1.04956442
19/32	1.0737935	1.0737935	1.23845668	1.14158378	1.08406539
21/32	1.12171569	1.12171569	1.3140076	1.20606767	1.13523194
23/32	1.19181797	1.19181797	1.40326325	1.28984572	1.20832665
25/32	1.2910383	1.2910383	1.50719168	1.39624385	1.30956557
27/32	1.42763075	1.42763075	1.62674006	1.52881239	1.44618555
29/32	1.61127988	1.61127988	1.76283673	1.69132139	1.62651014
31/32	1.85321519	1.85321519	1.916393	1.88775649	1.86001428

Table 8. Absolute error of HWCM of Example 3 for $\sigma = 1$.

Resolution (J)	3	4	5	6	7	8
HWCM error	2.2204×10^{-16}	4.4409×10^{-16}	2.2204×10^{-16}	4.4409×10^{-16}	4.4409×10^{-16}	2.2204×10^{-16}
CPU time (seconds)	0.947930	1.152302	1.580108	3.506233	14.581024	96.118520

Table 9. Absolute error of HWCM of Example 3 for different σ.

Resolution	3	4	5	6	7
$\sigma = 0.55$	9.6373×10^{-7}	8.6165×10^{-7}	8.8235×10^{-7}	8.924×10^{-7}	8.9734×10^{-7}
$\sigma = 0.75$	1.5783×10^{-7}	1.6771×10^{-7}	1.7277×10^{-7}	1.7534×10^{-7}	1.7663×10^{-7}
$\sigma = 0.95$	2.855×10^{-8}	3.0805×10^{-8}	3.1984×10^{-8}	3.2587×10^{-8}	3.2891×10^{-8}

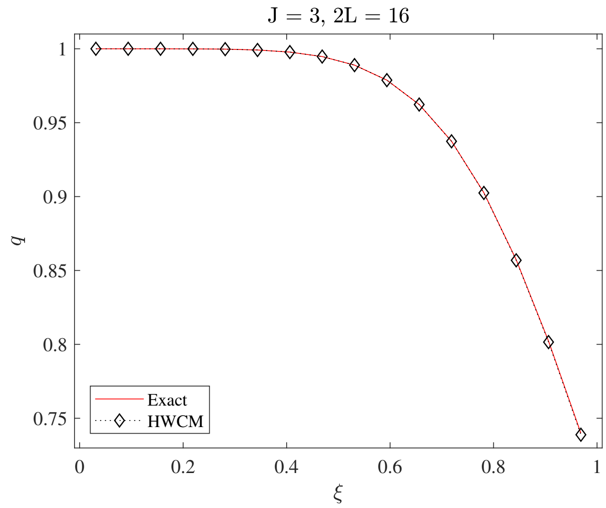

Figure 13. Comparison of Exact and HWCM solution of Example 4 when $\sigma = 1$.

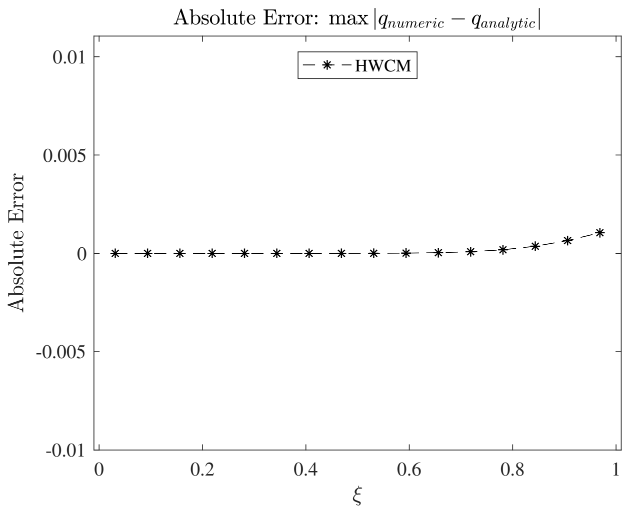

Figure 14. Absolute error of HWCM of Example 4 when σ = 1.

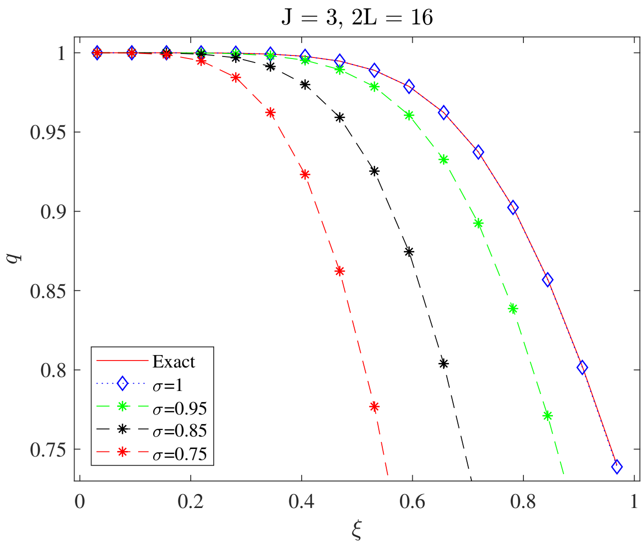

Figure 15. HWCM solution of Example 4 for different values of σ.

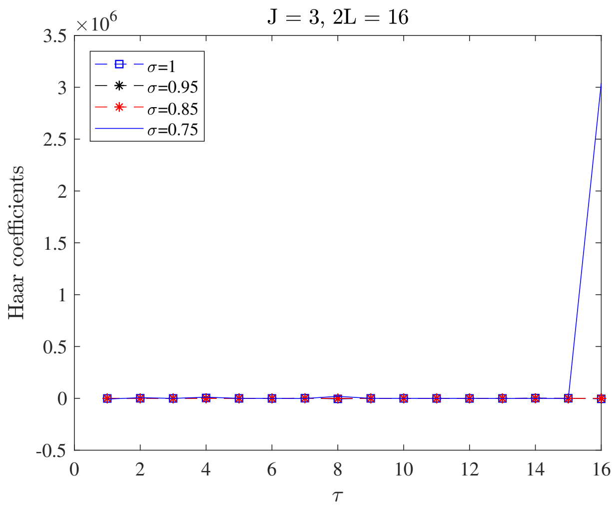

Figure 16. Haar coefficients of Example 4 for different values of σ.

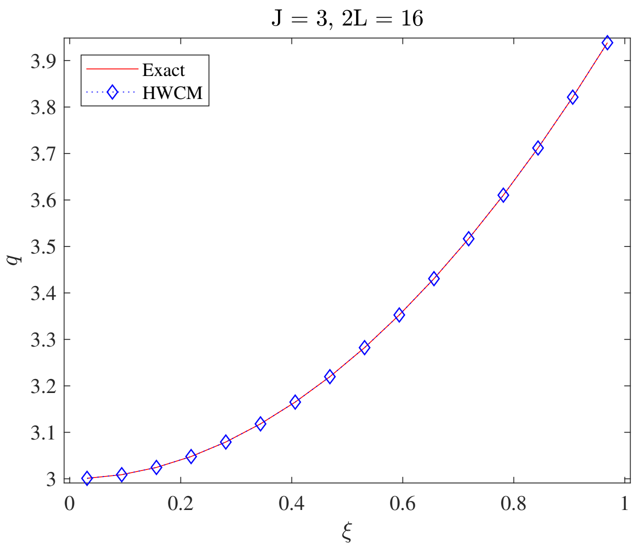

Figure 17. Comparison of Exact and HWCM solution of Example 5 when $\sigma = 1$.

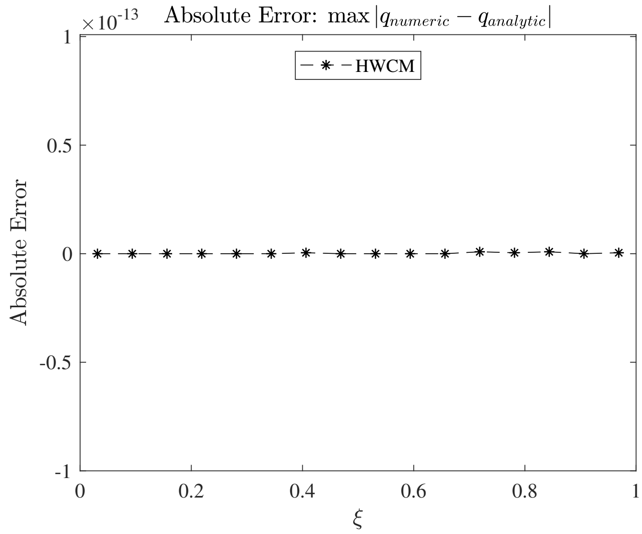

Figure 18. Absolute error of HWCM of Example 5 when $\sigma = 1$.

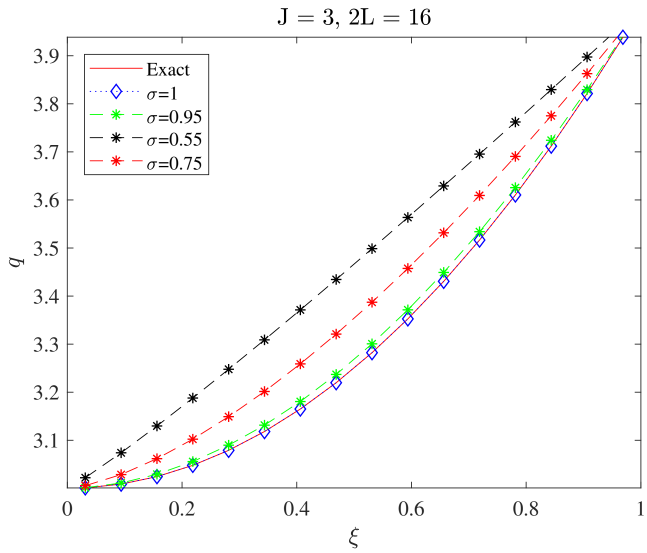

Figure 19. HWCM solution of Example 5 for different values of σ.

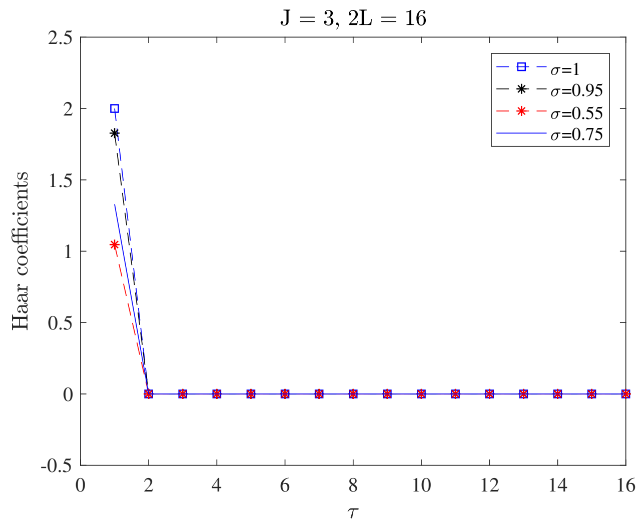

Figure 20. Haar coefficients of Example 5 for different values of σ.

Table 10. Comparison of HWCM and exact solution of Example 5 for J = 3.

ξ/32	Haar Solution	Exact Solution	$\sigma = 0.55$	$\sigma = 0.75$	$\sigma = 0.95$
1/32	3.000977	3.000977	3.022097	3.005524	3.001381
3/32	3.008789	3.008789	3.073989	3.028705	3.011136
5/32	3.024414	3.024414	3.129778	3.061763	3.029394
7/32	3.047852	3.047852	3.187907	3.102311	3.055706
9/32	3.079102	3.079102	3.247743	3.149155	3.089800
11/32	3.118164	3.118164	3.308935	3.201541	3.131480
13/32	3.165039	3.165039	3.371255	3.258935	3.180596
15/32	3.219727	3.219727	3.434546	3.320931	3.237022
17/32	3.282227	3.282227	3.498688	3.387212	3.300655
19/32	3.352539	3.352539	3.563591	3.457515	3.371404
21/32	3.430664	3.430664	3.629182	3.531623	3.449192
23/32	3.516602	3.516602	3.695402	3.609350	3.533947
25/32	3.610352	3.610352	3.762200	3.690534	3.625606
27/32	3.711914	3.711914	3.829536	3.775034	3.724113
29/32	3.821289	3.821289	3.897373	3.862724	3.829414
31/32	3.938477	3.938477	3.965679	3.953493	3.941461

Table 11. Absolute error of HWCM of Example 5.

Resolution (J)	3	4	5	6	7	8
HWM error	1.3323×10^{-15}	1.3323×10^{-15}	1.3323×10^{-15}	8.8818×10^{-16}	8.8818×10^{-16}	8.881×10^{-16}
CPU time (seconds)	0.984097	1.105506	1.766658	5.013335	23.477339	163.859775

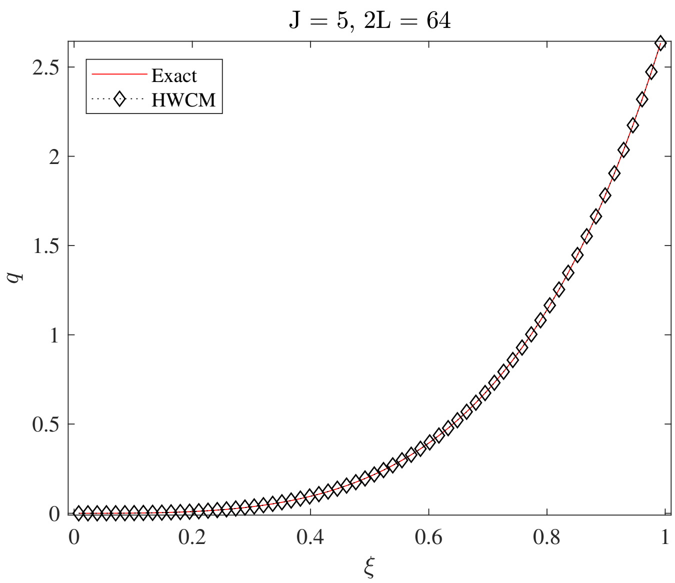

Figure 21. Comparison of Exact and HWCM solution of Example 6 when $\sigma = 1$.

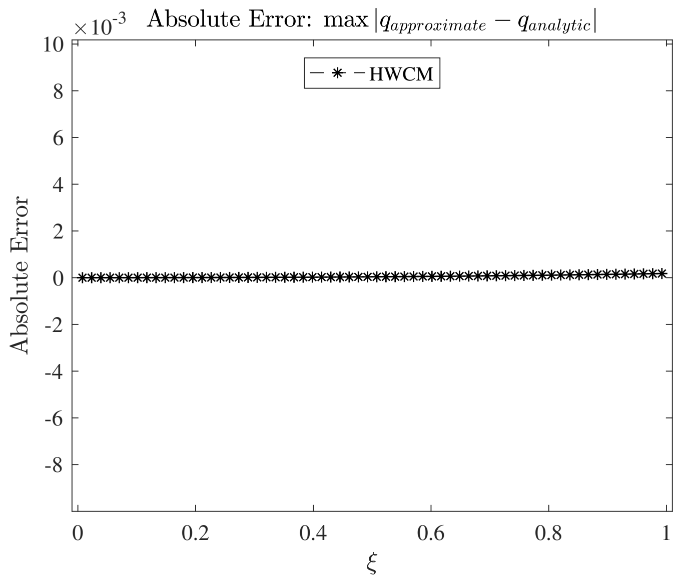

Figure 22. Absolute error of HWCM of Example 6 when $\sigma = 1$.

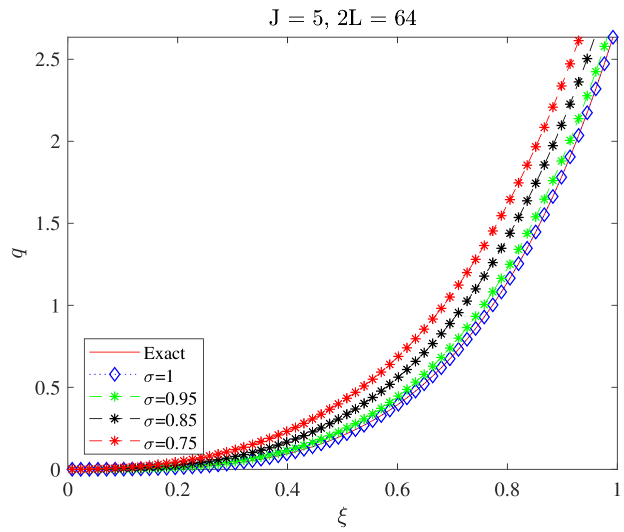

Figure 23. HWCM solution of Example 6 for different values of σ.

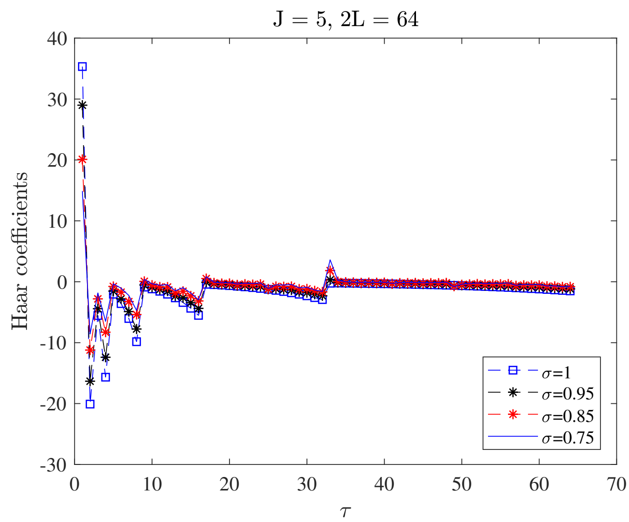

Figure 24. Haar coefficients of Example 6 for different values of σ.

Table 12. Comparison of HWCM and exact solution of Example 6 for J = 5.

ξ	Haar Solution	Exact Solution	Abs. Error	QBSM [39]	$\sigma = 0.75$	$\sigma = 0.85$	$\sigma = 0.95$
0.1	0.001103955	0.001105170	1.215×10^{-6}	0.001086890	0.010800993	0.004553355	0.001757272
0.2	0.009765978	0.009771222	5.244×10^{-6}	0.009734551	0.045949298	0.025702835	0.013439484
0.3	0.036433810	0.036446187	1.237×10^{-5}	0.036392585	0.115449927	0.075115699	0.046307124
0.4	0.095453799	0.095476780	2.298×10^{-5}	0.095408690	0.233442897	0.167418101	0.115047307
0.5	0.206052735	0.206090158	3.742×10^{-5}	0.206011349	0.415714680	0.320710379	0.238809970
0.6	0.393521515	0.393577660	5.614×10^{-5}	0.393493595	0.683319863	0.557181115	0.442071948
0.7	0.690637639	0.690717178	7.953×10^{-5}	0.690635447	1.071858878	0.908280793	0.756777190
0.8	1.139368842	1.139476955	1.081×10^{-4}	1.139407772	1.614156801	1.411098928	1.223361386
0.9	1.792908154	1.793050668	1.425×10^{-4}	1.793007437	2.350158149	2.109231858	1.891889010

Table 13. Absolute error of HWCM of Example 6 for σ = 1.

Resolution (J)	3	4	5	6	7	8
HWCM error	2.70×10^{-3}	7.0396×10^{-4}	1.7755×10^{-4}	4.2618×10^{-5}	8.5528×10^{-6}	1.5229×10^{-6}
$R_C(L)$	—	1.939394	1.987268	2.058690	2.316994	2.489575
CPU time (seconds)	0.985559	1.175652	1.641920	4.269479	19.495244	136.006084

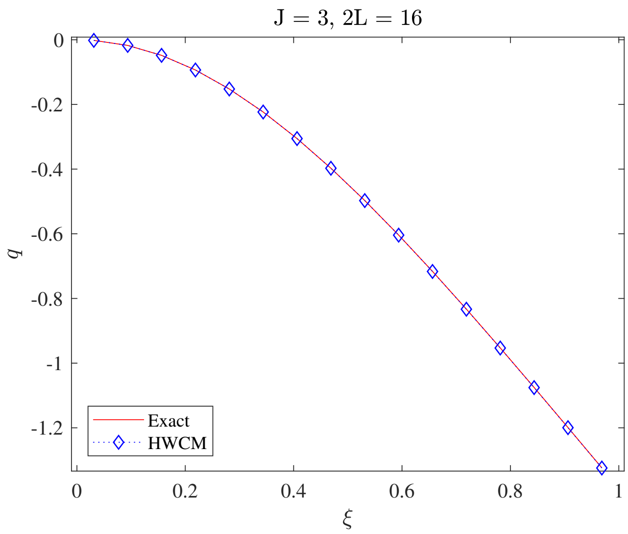

Figure 25. Comparison of Exact and HWCM solution of Example 4 when $\sigma = 1$.

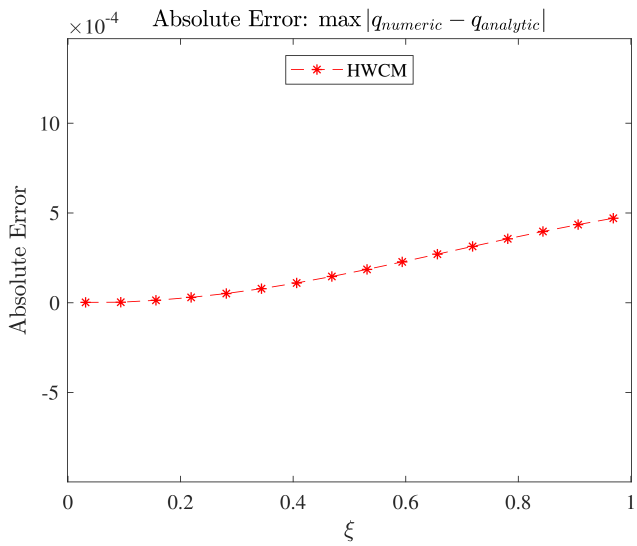

Figure 26. Absolute error of HWCM of Example 7 when σ = 1.

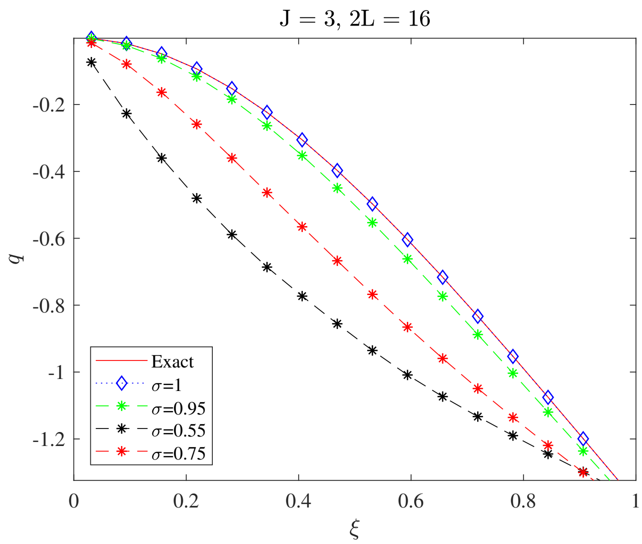

Figure 27. HWCM solution of Example 7 for different values of σ.

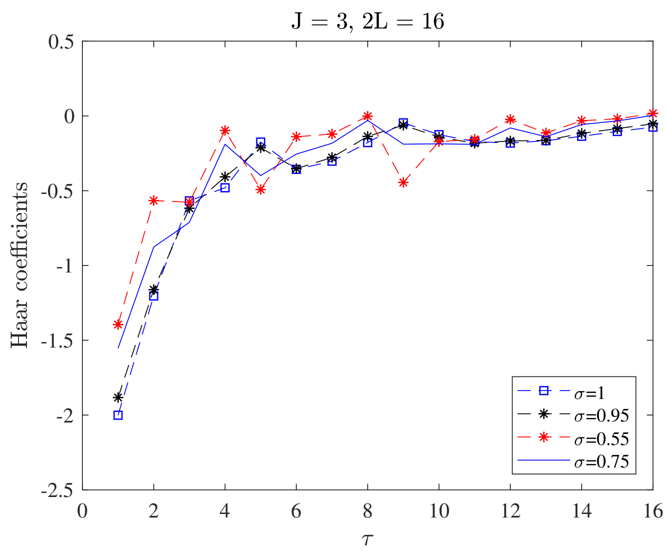

Figure 28. Haar coefficients of Example 7 for different values of σ.

Table 14. Comparison of HWCM and exact solution of Example 7 for J = 3.

ξ	Haar Solution	Exact Solution	Abs. Error	VIM [41]	$\sigma = 0.55$	$\sigma = 0.75$	$\sigma = 0.95$
0.1	−0.01990248	−0.01990066	8.95×10^{-5}	−0.01990066	−0.24073779	−0.08666051	−0.02698493
0.2	−0.07847532	−0.07844142	3.4×10^{-5}	−0.07844138	−0.44642869	−0.22954585	−0.09871719
0.3	−0.17240439	−0.17235539	4.9×10^{-5}	−0.17235319	−0.61995038	−0.39098635	−0.20674133
0.4	−0.29695266	−0.29684001	1.12×10^{-4}	−0.29680298	−0.76453325	−0.55548832	−0.34321737
0.5	−0.44645232	−0.44628710	1.65×10^{-4}	−0.44596354	−0.89619911	−0.71772963	−0.50067339
0.6	−0.61519627	−0.61496939	2.26×10^{-4}	−0.61310592	−1.01542342	−0.87501502	−0.67261708
0.7	−0.79786090	−0.79755223	3.08×10^{-4}	−0.78950866	−1.11575420	−1.02264092	−0.85328881
0.8	−0.98975390	−0.98939248	3.61×10^{-4}	−0.96127658	−1.20678787	−1.16109114	−1.03825098
0.9	−1.18708784	−1.18665369	4.34e-04	−1.10296039	−1.29291002	−1.29224026	−1.22443125

Table 15. Abs. error of HWCM of Example 7 for $\sigma = 1$.

Resolution (J)	3	4	5	6	7	8
HWCM error	4.70×10^{-4}	1.19×10^{-4}	3.0098×10^{-5}	7.5548×10^{-6}	1.8926×10^{-6}	4.7363×10^{-7}
$R_C(L)$	1.963964	1.978709	1.988404	1.992906	1.998703	1.998537
CPU time (seconds)	2.388590	1.868506	2.802558	7.324519	33.503430	196.555354

Author Contributions: P.G. led the study and organized the required literature. A.K. wrote the manuscript, interpreted the results and conducted all the numerical calculations and made the graphs. K.S.A. and B.S.A. summarized the data for tables, created the study site map, and formatted the final document. All authors have read and agreed to the published version of the manuscript.

Funding: This work was supported and funded by the Deanship of Scientific Research at Imam Mohammad Ibn Saud Islamic University (IMSIU) (grant number IMSIU-RP23028).

Institutional Review Board Statement: Not applicable.

Informed Consent Statement: Not applicable.

Data Availability Statement: Not applicable.

Acknowledgments: The authors extend their appreciation to the Deanship of Scientific Research at Imam Mohammad Ibn Saud Islamic University (IMSIU) (grant number IMSIU-RP23028) for funding and supporting this work. Ashish Kumar is also thankful to UGC for providing a Junior Research Fellowship.

Conflicts of Interest: Researchers state that there are no conflict of interest to report regarding the presented article.

References

1. Lane, H.J. On the theoretical temperature of the sun, under the hypothesis of a gaseous mass maintaining its volume by its internal heat, and depending on the laws of gases as known to terrestrial experiment. *Am. J. Sci.* **1870**, *2*, 57–74. [CrossRef]
2. Fowler, R. Some results on the form near infinity of real continuous solutions of a certain type of second order differential equation. *Proc. Lond. Math. Soc.* **1914**, *2*, 341–371. [CrossRef]
3. Chandrasekhar, S. *An Introduction to the Study of Stellar Structure*; Dover Publications: New York, NY, USA, 1957.
4. Dehghan, M.; Shakeri, F. Solution of an integro-differential equation arising in oscillating magnetic fields using He's homotopy perturbation method. *Prog. Electromagn. Res.* **2008**, *78*, 361–376. [CrossRef]
5. Ramos, J.I. Linearization methods in classical and quantum mechanics. *Comput. Phys. Commun.* **2003**, *153*, 199–208. [CrossRef]
6. Bhrawy, A.; Alofi, A.; Van Gorder, R. An efficient collocation method for a class of boundary value problems arising in mathematical physics and geometry. *Abstr. Appl. Anal.* **2014**, *2014*, 425648. [CrossRef]
7. Boubaker, K.; Van Gorder, R.A. Application of the BPES to Lane–Emden equations governing polytropic and isothermal gas spheres. *New Astron.* **2012**, *17*, 565–569. [CrossRef]
8. Flockerzi, D.; Sundmacher, K. On coupled Lane-Emden equations arising in dusty fluid models. *J. Phys. Conf. Ser.* **2011**, *268*, 012006. [CrossRef]
9. He, J. Nonlinear oscillation with fractional derivative and its applications. In Proceedings of the International Conference on Vibrating Engineering, Dalian, China, 6–9 August 1998; Volume 98, pp. 288–291.
10. Alzabut, J.; Tyagi, S.; Abbas, S. Discrete fractional-order BAM neural networks with leakage delay: Existence and stability results. *Asian J. Control* **2020**, *22*, 143–155. [CrossRef]
11. Pratap, A.; Raja, R.; Alzabut, J.; Dianavinnarasi, J.; Cao, J.; Rajchakit, G. Finite-time Mittag-Leffler stability of fractional-order quaternion-valued memristive neural networks with impulses. *Neural Process. Lett.* **2020**, *51*, 1485–1526. [CrossRef]
12. Panda, R.; Dash, M. Fractional generalized splines and signal processing. *Signal Process.* **2006**, *86*, 2340–2350. [CrossRef]
13. Baillie, R.T. Long memory processes and fractional integration in econometrics. *J. Econom.* **1996**, *73*, 5–59. [CrossRef]
14. Magin, R. Fractional calculus in bioengineering, part 1. *Crit. Rev. Trade Biomed. Eng.* **2004**, *32*, 1–104. [CrossRef]
15. Engheta, N. On fractional calculus and fractional multipoles in electromagnetism. *IEEE Trans. Antennas Propag.* **1996**, *44*, 554–566. [CrossRef]
16. Al-Khaled, K.; Momani, S. An approximate solution for a fractional diffusion-wave equation using the decomposition method. *Appl. Math. Comput.* **2005**, *165*, 473–483. [CrossRef]
17. Al-Mdallal, Q.M.; Syam, M.I.; Anwar, M. A collocation-shooting method for solving fractional boundary value problems. *Commun. Nonlinear Sci. Numer. Simul.* **2010**, *15*, 3814–3822. [CrossRef]
18. Alquran, M.; Al-Khaled, K.; Chattopadhyay, J. Analytical solutions of fractional population diffusion model: Residual power series. *Nonlinear Stud.* **2015**, *22*, 31–39.

19. Jaradat, H.; Al-Shara, S.; Khan, Q.J.; Alquran, M.; Al-Khaled, K. Analytical solution of time-fractional Drinfeld-Sokolov-Wilson system using residual power series method. *IAENG Int. J. Appl. Math.* **2016**, *46*, 64–70.
20. Meerschaert, M.M.; Tadjeran, C. Finite difference approximations for two-sided space-fractional partial differential equations. *Appl. Numer. Math.* **2006**, *56*, 80–90. [CrossRef]
21. Das, S. Analytical solution of a fractional diffusion equation by variational iteration method. *Comput. Math. Appl.* **2009**, *57*, 483–487. [CrossRef]
22. Zhang, H.; Han, X. Quasi-wavelet method for time-dependent fractional partial differential equation. *Int. J. Comput. Math.* **2013**, *90*, 2491–2507. [CrossRef]
23. Jiang, X.; Wang, J.; Wang, W.; Zhang, H. A Predictor–Corrector Compact Difference Scheme for a Nonlinear Fractional Differential Equation. *Fractal Fract.* **2023**, *7*, 521. [CrossRef]
24. Yang, X.; Wu, L.; Zhang, H. A space-time spectral order sinc-collocation method for the fourth-order nonlocal heat model arising in viscoelasticity. *Appl. Math. Comput.* **2023**, *457*, 128192. [CrossRef]
25. Guf, J.S.; Jiang, W.S. The Haar wavelets operational matrix of integration. *Int. J. Syst. Sci.* **1996**, *27*, 623–628. [CrossRef]
26. Díaz, L.A.; Martín, M.T.; Vampa, V. Daubechies wavelet beam and plate finite elements. *Finite Elem. Anal. Des.* **2009**, *45*, 200–209. [CrossRef]
27. ur Rehman, M.; Khan, R.A. The Legendre wavelet method for solving fractional differential equations. *Commun. Nonlinear Sci. Numer. Simul.* **2011**, *16*, 4163–4173. [CrossRef]
28. Lepik, Ü. Numerical solution of evolution equations by the Haar wavelet method. *Appl. Math. Comput.* **2007**, *185*, 695–704. [CrossRef]
29. Chen, C.F.; Hsiao, C.H. Haar wavelet method for solving lumped and distributed-parameter systems. *IEE Proc.-Control Theory Appl.* **1997**, *144*, 87–94. [CrossRef]
30. Lepik, Ü. Numerical solution of differential equations using Haar wavelets. *Math. Comput. Simul.* **2005**, *68*, 127–143. [CrossRef]
31. ul Islam, S.; Aziz, I.; Fayyaz, M. A new approach for numerical solution of integro-differential equations via Haar wavelets. *Int. J. Comput. Math.* **2013**, *90*, 1971–1989. [CrossRef]
32. Bujurke, N.; Salimath, C.; Shiralashetti, S. Computation of eigenvalues and solutions of regular Sturm–Liouville problems using Haar wavelets. *J. Comput. Appl. Math.* **2008**, *219*, 90–101. [CrossRef]
33. Chang, P.; Piau, P. Haar wavelet matrices designation in numerical solution of ordinary differential equations. *IAENG Int. J. Appl. Math.* **2008**, *38*, 1–5.
34. Ray, S.S. On Haar wavelet operational matrix of general order and its application for the numerical solution of fractional Bagley Torvik equation. *Appl. Math. Comput.* **2012**, *218*, 5239–5248.
35. Sun, H.; Mei, L.; Lin, Y. A new algorithm based on improved Legendre orthonormal basis for solving second-order BVPs. *Appl. Math. Lett.* **2021**, *112*, 106732. [CrossRef]
36. LeVeque, R.J. *Finite Difference Methods for Ordinary and Partial Differential Equations: Steady-State and Time-Dependent Problems*; SIAM: Philadelphia, PA, USA, 2007.
37. Ali, K.K.; Mehanna, M.; Abdelrahman, M.I.; Shaalan, M. Analytical and numerical solutions for fourth order Lane–Emden–Fowler equation. *Partial. Differ. Equ. Appl. Math.* **2022**, *6*, 100430. [CrossRef]
38. Syam, M.I. Analytical solution of the fractional initial Emden–Fowler equation using the fractional residual power series method. *Int. J. Appl. Comput. Math.* **2018**, *4*, 106. [CrossRef]
39. Iqbal, M.K.; Abbas, M.; Wasim, I. New cubic B-spline approximation for solving third order Emden–Flower type equations. *Appl. Math. Comput.* **2018**, *331*, 319–333. [CrossRef]
40. Mohammadi, A.; Ahmadnezhad, G.; Aghazadeh, N. Chebyshev-quasilinearization method for solving fractional singular nonlinear Lane-Emden equations. *Commun. Math.* **2022**, *30*. [CrossRef]
41. Yıldırım, A.; Öziş, T. Solutions of singular IVPs of Lane–Emden type by the variational iteration method. *Nonlinear Anal. Theory Methods Appl.* **2009**, *70*, 2480–2484. [CrossRef]